Supporting Information

NHPI-Mediated Electrochemical Iodination of Methylarenes and Comparison to Electron-Transfer-Initiated C–H Functionalization

Mohammad Rafiee, Fei Wang, Damian P. Hruszkewycz, and Shannon S. Stahl*

Department of Chemistry, University of Wisconsin−Madison, 1101 University Avenue, Madison, WI 53706, United States

Table of Contents

1. General Considerations.

All chemicals and solvents were purchased from commercially available sources and used without further purification. Dry solvents were obtained from a solvent purification system using columns of Al_2O_3 under argon. ^{1}H, ^{13}C and ^{19}F NMR spectra were obtained with Bruker Avance-400 MHz with residual solvent peaks or tetramethylsilane as the internal reference. Multiplicities are described using the following abbreviations: s = singlet, bs = broad singlet, d = doublet, dd = doublet of doublet, t = triplet, m = multiplet. Chromatography was performed using an automated Biotage Isolera® with reusable 120 g or 60 g Biotage® SNAP Ultra C-18 cartridges or standard silica cartridges. High-resolution mass spectra were obtained using a Thermo Q Exactive™ Plus via (ASAP-MS) by the mass spectrometry facility at the University of Wisconsin (funded by NIH grant: 1S10OD020022-1). The supporting electrolytes ($PyH^+ClO_4^-$ = Pyridinium Perchlorate; 2,6-$LutH^+ClO_4^-$ = 2,6-Lutidinium Perchlorate; 2,6-DTBP$yH^+ClO_4^-$ = 2,6-di-^{t}BuPyridinium Perchlorate) were prepared according to the reported procedures[1] and dried under vacuum overnight before its usage. Voltammetric experiments were performed using a Pine potentio/galvanostat model Wavenow. Bulk electrolysis reactions were performed using a Nuvant Array PGStats, from Nuvant System Inc.

2. CV Study under Different Conditions

For all the voltammetric experiments, a disc electrode (2 mm diameter) and a platinum wire were used as working and counter electrodes, respectively. The working electrode potentials were measured versus $Ag/AgNO_3$ reference electrode (internal solution 0.1 M Bu_4NClO_4 and 0.01 M $AgNO_3$ in CH_3CN,). The redox potential of ferrocene/ ferrocenium (Fc/Fc^+) was measured (under the same experimental conditions) and used to provide an internal reference potential calibration. The potential values were then adjusted relative to the Fc/Fc^+ potential electrochemical studies in organic solvents.

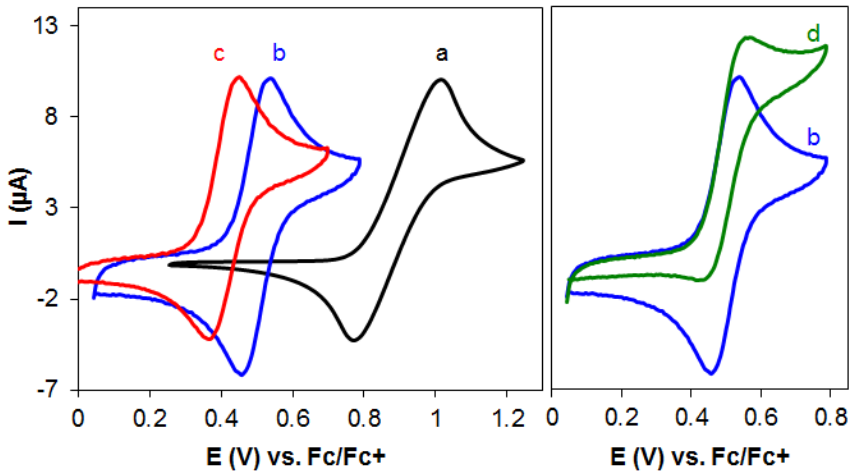

Figure S1. CVs of NHPI (1 mM) in acetonitrile (**a**); in the presence of pyridine/pyridinium perchlorate (0.1 M each) (**b**); pyridine (0.01 M) and solid $KHCO_3$ (100 equiv) (**c**); and in the presence of pyridine/pyridinium perchlorate (0.1 M each), and 4-^{t}Bu-toluene (20 mM) (**d**). Other conditions: glassy carbon working electrode (~ 7.0 mm^2), scan rate = 10 mV/s, and 0.1 M KPF_6 electrolyte for (**a**) and (**c**).

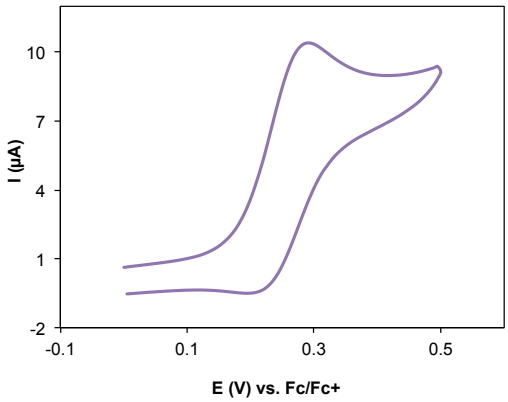

Figure S2. Cyclic voltammograms of NHPI (1 mM) in acetonitrile in the presence of 0.1 M tetrabutylammonium acetate at glassy carbon working electrode (~ 7.0 mm^2), scan rate = 10 mV/s.

The cathodic-to-anodic peak-current ratio differs under various conditions. These results show that PINO is unstable under basic conditions.

3. Evaluation of Different Radical Traps

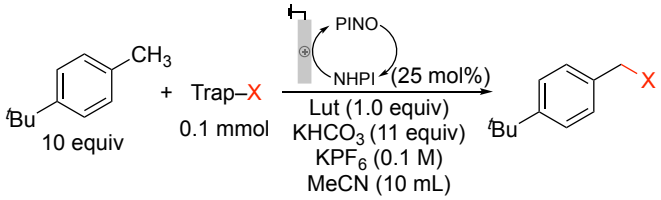

Trap–X	PhSSPh	TsCN	TsC≡CPh	$CuCl_2$	I_2 (0.5 equiv)
Yield	0%	0%	0%	0%	100%

Scheme S1. Evaluation of different radical traps

These reactions were carried out using an H-type divided cell equipped with a reticulated vitreous carbon anode (RVC, 30 PPI, 4.0 cm x 1.0 cm x 0.6 cm, ~ 3.0 cm was immersed in the solution) and a platinum wire cathode (1.0 cm, spiral wire). In the anodic chamber, 4-^{t}Bu-toluene (1.0 mmol, 10 equiv), NHPI (0.025 mmol, 25 mol%), Trap-X (0.1 mmol, 1.0 equiv), 2,6-Lutidine (0.1 mmol, 1.0 equiv), $KHCO_3$ (1.1 mmol, 11 equiv), KPF_6 (0.1 M) were dissolved in CH_3CN (10.0 mL). In the cathodic chamber was placed KPF_6 (0.1 M) and CH_3CN (10.0 mL). Constant current electrolysis (5 mA) was carried out at room temperature with magnetic stirring. The applied potential was tracked with the cutoff potential at 1.2 V vs Ag/Ag^+ (1.12 V vs Fc/Fc^+). After that, these reactions were analyzed by ^{1}H NMR spectroscopy.

4. Optimization of the Reaction Conditions

a) Evaluation of currents and potentials.

Reactions were performed in a divided cell according to "Conditions A" described in section 5 below.

Table S1. Optimization of electrochemical parameters for bulk electrolysis

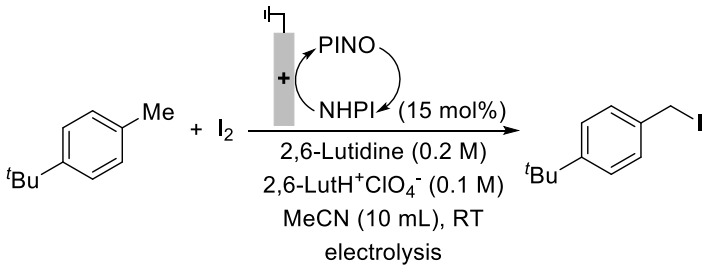

entry	Electrolysis Condition	Time (min)	% yield
1	Constant potential at 0.70 V vs. Ag/Ag^+ (0.63 V vs Fc/Fc^{+}) [a]	150	31%
2	Constant current at 15 mA [b]	130	28%
3	Constant current at 10 mA [b]	190	39%
4	Constant current at 5 mA [b]	310	52%
5	Constant current at 3 mA [b]	490	46%

[a:] This applied potential is higher than peak potential observed by cyclic voltammetry; the peak potential under these conditions was 0.55 V vs. Ag/Ag^+ (0.48 V vs Fc/Fc^+). The initial current was 21 mA and the reaction was terminated when the current reached 1 mA. [b:] The reactions were terminated when the potential reached to 1.2 V 1.20 V vs. Ag/Ag^+ (1.12 V vs Fc/Fc^+).

b) Testing of undivided cell configuration.

The reaction conditions defined in entry 4 of Table S1 were tested in a ca. 15 mL undivided cell. Considerably lower yields were obtained: 16% and 19% product after 480 and 600 minutes, respectively. The poor results are rationalized by facile redox cycling of the I_2/I^- redox couple at the anode and cathode, which limits productive use of current.

c) Effect of supporting electrolyte

Different anions, including ClO_4^-, PF_6^- and BF_4^- were examined as the counterion of 2,6-lutidinium for bulk electrolysis reactions. NMR yields were similar for each of these counterions. **Caution**: organic perchlorate salts can be explosive.

Table S2. Evaluation of catalyst and iodine loading

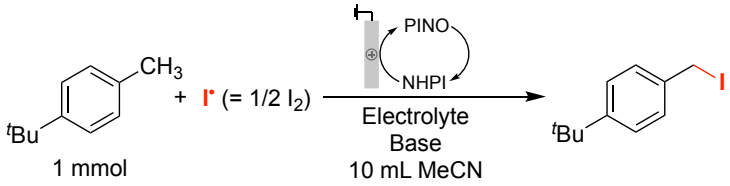

entry	NHPI (mol%)	Base (equiv)	Electrolyte (equiv)[a]	I• (equiv)	% yield
1	20%	Lut (1.5)	[LutH]**ClO_4** (1.0)	1.0	57
2	20%	Lut (1.5)	[LutH]**PF_6** (1.0)	1.0	55
3	20%	Lut (1.5)	[LutH]**BF_4** (1.0)	1.0	54

The cationic portion of the electrolyte also has an influence on the reaction. For example, use of 2,6-DTBPyH$^+$ClO$_4^-$ instead of LutH$^+$ClO$_4^-$ as the supporting electrolyte resulted in higher yields for some of the substrates. Lutidinium can displace iodide from some of the benzylic iodide products, and lutidine can undergo iodination of the benzylic methyl groups under the reaction conditions. For example, Figure S3 shows the formation of benzyllutidinium and the iodination product of lutidine during the iodination reaction of 4-chlorotoluene. Figure S4 shows a crude NMR spectrum from an electrolysis reaction under Conditions A (see section 5, below) in the absence of a methylarene substrate, but containing 0.3 M 2,6-lutidine.

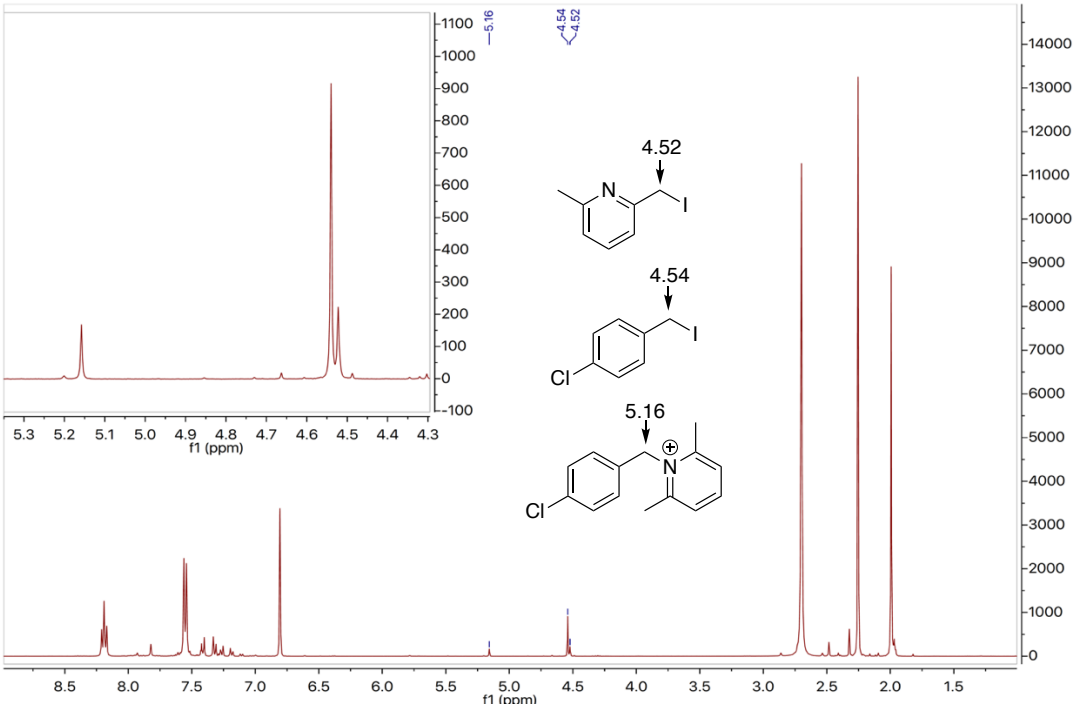

Figure S3. Crude NMR spectrum obtained from the reaction mixture for iodination of 4-chlorotoluene under Conditions A.

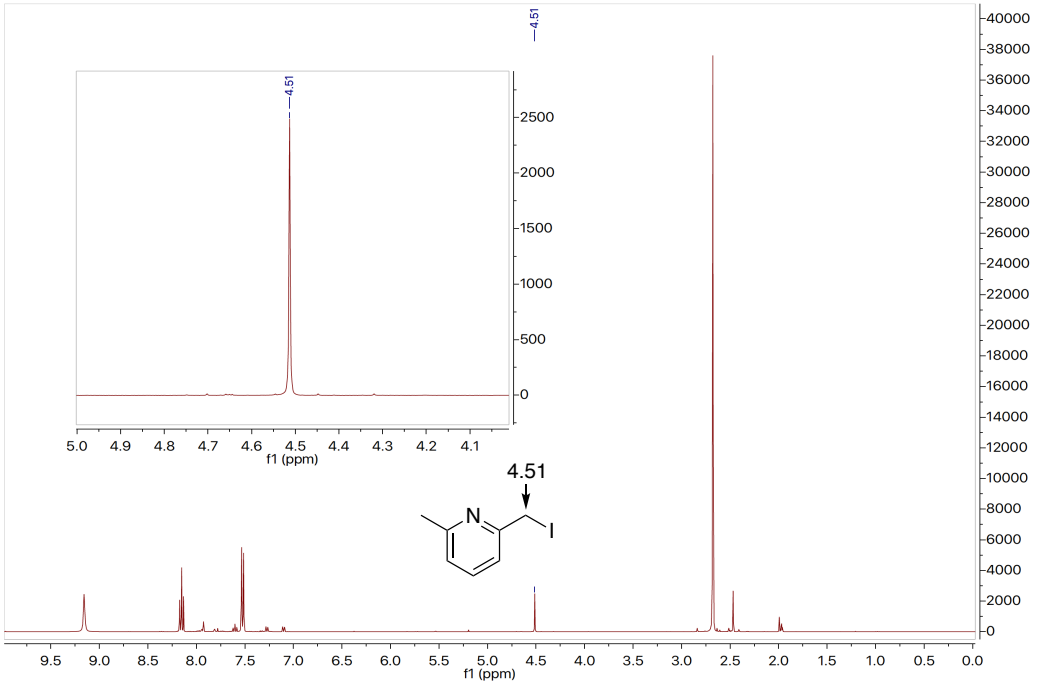

Figure S4. Crude NMR spectrum obtained from the reaction mixture under Conditions A in absence of a methylarene substrate, but containing 0.3 M 2,6-lutidine.

d) Effect of base (see also, Table 1 of the manuscript, for additional data)

Table S3. Evaluation of catalyst and iodine loading

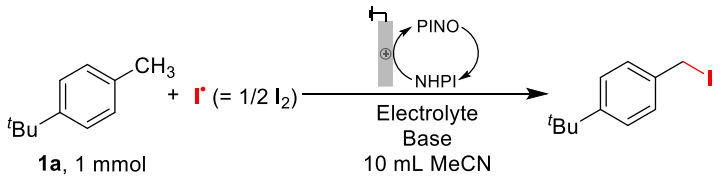

entry	NHPI (mol%)	Base (equiv)	Electrolyte	I• (equiv)	% yield vs $ArCH_3$ (vs I•)
1	2.5%	Lut, $KHCO_3$ (0.1, 1.1)	KPF_6	0.1	10 (100)
2	2.5%	Lut, $KHCO_3$ (0.1, 1.1)	KPF_6	0.3	26 (86)
3	7.5%	Lut, $KHCO_3$ (0.1, 1.1)	KPF_6	0.3	28 (92)
4	7.5%	Lut, $KHCO_3$ (0.1, 3.3)	KPF_6	0.5	36 (72)
5	15%	Lut, $KHCO_3$ (0.1, 3.3)	KPF_6	1.0	38 (38)

e) Effect of Electrode Material

Voltammetric study of the NHPI and methyarene oxidation were studied using different electrode materials. CVs of 4-chlorotoluene are shown in Figure S5. Glassy carbon was used as the electrode for further voltammetric studies and bulk electrolysis reactions (RVC). The observed redox potentials are comparable to those reported in the literature.[2,3]

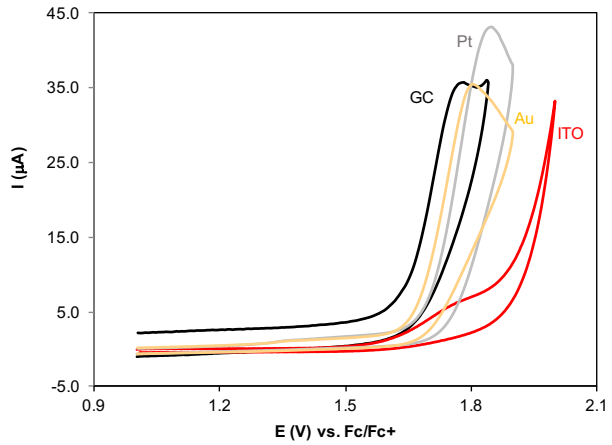

Figure S5. CVs of 4-chlorotoluene in acetonitrile and in the presence of pyridine/pyridinium perchlorate (0.1 M each) at the surface of Glassy Carbon (GC), Platinum (Pt), Gold (Au) and Indium Tin Oxide (ITO). Scan rate 10 mVs^{-1}, electrode surface area ~ 7.0 mm^2.

f) Evaluation of mediators

Voltammetry and chronoamperometry were used after bulk electrolysis to probe the stability of different imidoxyl radicals. Figure S6 shows the voltammograms of NHPI and Cl_4NHPI before and after a 10 min bulk electrolysis, recorded using a rotating disc electrode (the current is proportional to the bulk concentration of electroactive species). These results show that concentration of PINO (Figure S6-A) is higher than Cl_4PINO (Figure S6-B), and are indicative of the higher stability of PINO under these conditions. When NHSI was subjected to the same conditions, no reduction current was detected after bulk electrolysis, demonstrating the instability of SINO.

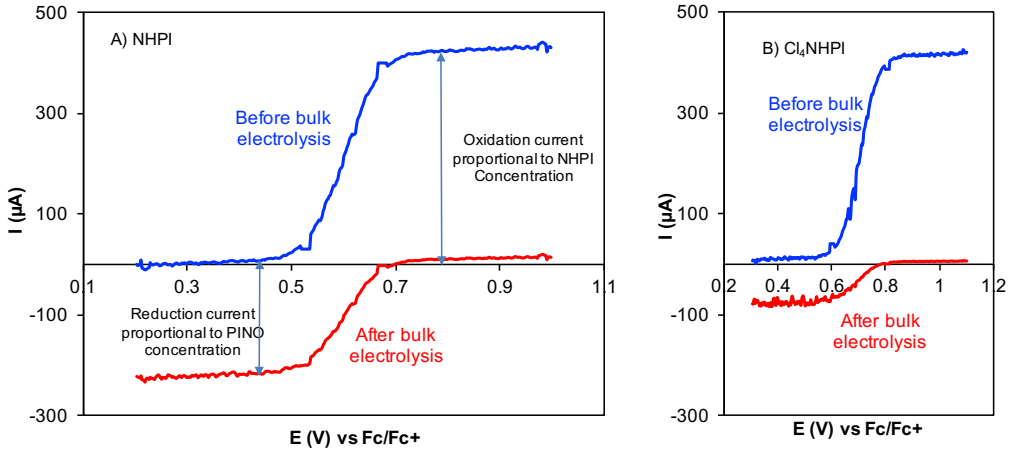

Figure S6. Linear sweep voltammograms of NHPI (A) and Cl_4NHPI (B) before and after bulk electrolysis. reaction condition: 5 mM of each catalyst in MeCN including 0.1 M Py, 0.1 M $PyH^+ClO_4^-$. Glassy carbon electrode (~ 7.0 mm^2), rotation rate: 500 rpm.

Chronoamperometry was used to probe the stability of imidoxyl species generated by electrolysis by measuring the cathodic current at constant potential (0.22 V vs Fc/Fc^+; cf. Figure S6). The time courses reveal the half-life of PINO is ~ 4 min, while Cl_4PINO is ~ 40 s.

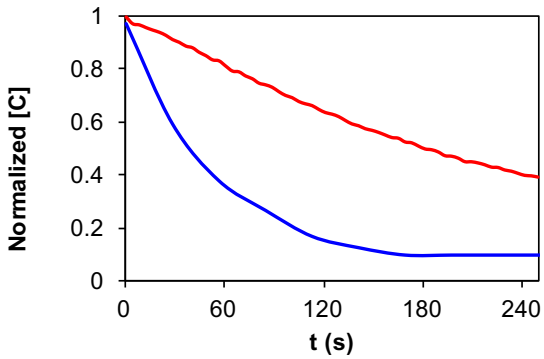

Figure S7. Concentration profiles of PINO (electrochemically generated from NHPI) (red) and Cl_4PINO (electrochemically generated from Cl_4NHPI) (blue). The currents are normalized based on the initial concentration of PINO after bulk electrolysis.

The reactivity of these mediators was also evaluated by bulk electrolysis with 2-bromotoluene as the substrate, in which NHPI lasted 2 and 4 h longer than Cl_4NHPI and NHSI respectively and gave the best yield (68%). The yields with NHSI and Cl_4NHPI were only 28% and 51% with a significant amount of starting material intact.

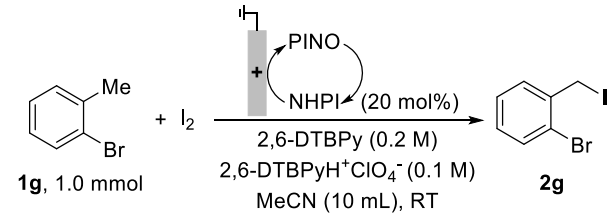

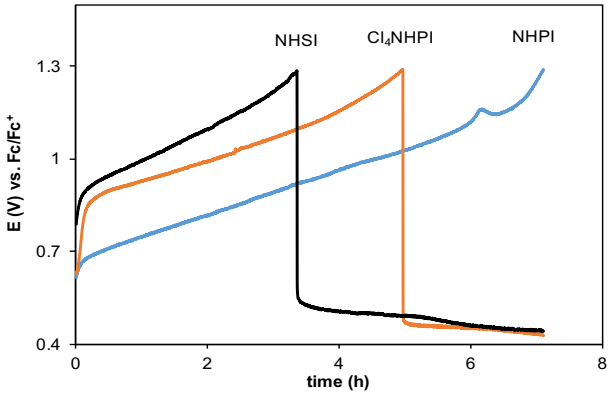

Figure S8. Bulk electrolysis plots for iodination of 2-bromotoluene catalyzed by NHPI, Cl_4NHPI and NHSI. Reaction conditions: anodic compartment: 0.1 M 2-bromotoluene, 20 mol% catlyst, 50 mol% I_2, 0.2 M 2,6-DTBPy, 0.1 M 2,6-DTBPyH$^+$ClO$_4^-$, 10 mL MeCN, 5 mA; cathodic compartment: 0.2 M 2,6-DTBPyH$^+$ClO$_4^-$ in 10 mL MeCN.

g) The effect of supporting electrolyte of cathodic compartment.

Figure S9 depicts the anodic reaction (generation of PINO and LutH$^+$), cathodic reaction (H_2 evolution and consumption of LutH$^+$) and ion transfer through the membrane during bulk electrolysis.

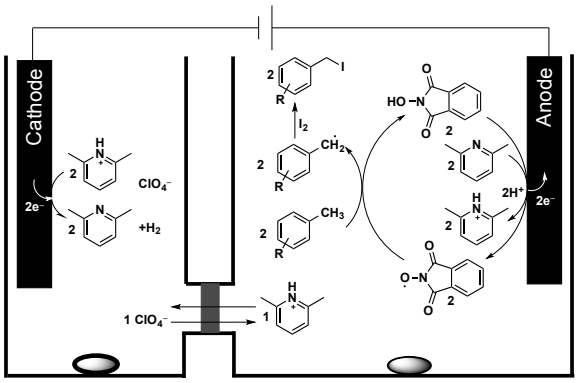

Figure S9. Schematic presentation of anodic and cathodic reactions for the divided electrochemical cell.

5. General Procedures for Electrochemical Functionalization of Methylarenes: Iodination of Methylarenes

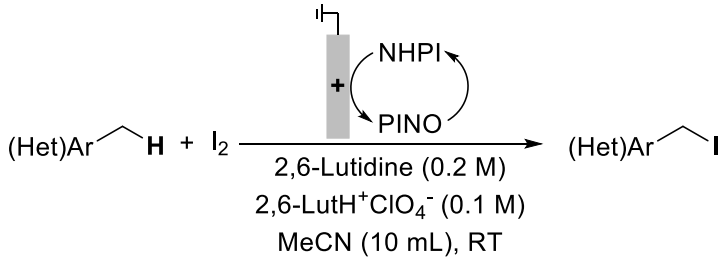

Conditions A: The reaction was carried out using an H-type divided cell (see Figure S10) equipped with a reticulated vitreous carbon anode (RVC, 30 PPI, 4.0 cm x 1.0 cm x 0.6 cm, ~ 3.0 cm was immersed in the solution) and a platinum wire cathode (1.0 cm, spiral wire). In the anodic chamber, methylarene (1.0 mmol), NHPI (0.2 mmol, 20 mol%), I_2 (0.50 mmol, 50 mol%), 2,6-lutidine (2.0 mmol, 0.2 M) and 2,6-Lut$H^+ClO_4^-$ (1.0 mmol, 0.1 M) were dissolved in CH_3CN (10.0 mL). In the cathodic chamber was placed 2,6-Lut$H^+ClO_4^-$ (2.0 mmol, 0.2 M) and CH_3CN (10.0 mL). Constant current electrolysis (5 mA/mmol) was carried out at room temperature with magnetic stirring. The reactions were terminated when the potentials reached 1.20 V vs. Ag/Ag^+ (1.12 V vs Fc/Fc^+) (This cutoff potential corresponds to the lowest redox potential at which one of the methylarene could undergo direct electron transfer). The average reaction time was 7 h for the substrates listed in substrate scope table. The solvent from both cell compartments was removed under vacuum, and the residue was purified by column chromatography on silica gel with a gradient eluent of pentane and ethyl acetate to give the product.

Conditions B: The reaction was carried out using an H-type divided cell equipped with a reticulated vitreous carbon anode (RVC, 30 PPI, 4.0 cm x 1.0 cm x 0.6 cm, ~ 3.0 cm was immersed in the solution) and a platinum wire cathode (1.0 cm, spiral wire). In the anodic chamber, methylarene (1.0 mmol), NHPI (0.2 mmol, 20 mol%), I_2 (0.50 mmol, 50 mol%), 2,6-di-^{t}BuPyridine (2.0 mmol, 0.2 M) and 2,6-DTBPy$H^+ClO_4^-$ (1.0 mmol, 0.1 M) were dissolved in CH_3CN (10.0 mL). In the cathodic chamber was placed 2,6-DTBPy$H^+ClO_4^-$ (2.0 mmol, 0.2 M) and CH_3CN (10.0 mL). Constant current electrolysis (5 mA/mmol) was carried out at room temperature with magnetic stirring. The reactions were terminated when the potentials reached to 1.20 V vs. Ag/Ag^+ (1.12 V vs Fc/Fc^+). The average reaction time was 7 hours for the substrates listed in substrate scope table. The solvent from both cell compartments was removed under vacuum, and the residue was purified by column chromatography on silica gel with a gradient eluent of pentane and ethyl acetate to give the product.

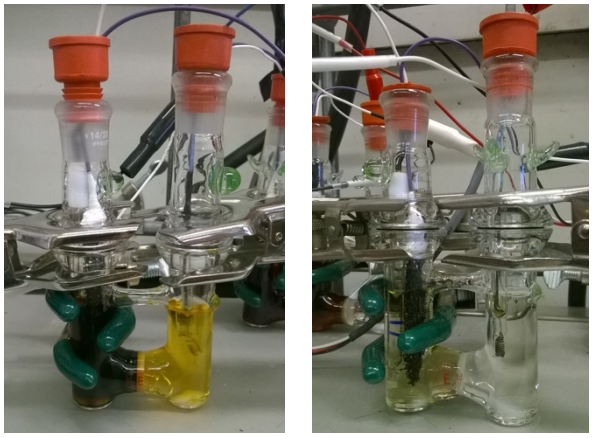

Figure S10. H-type divided cell for electrolysis. Left: before bulk electrolysis; Right: after bulk electrolysis.

6. Benzyl Pyridinium Formation

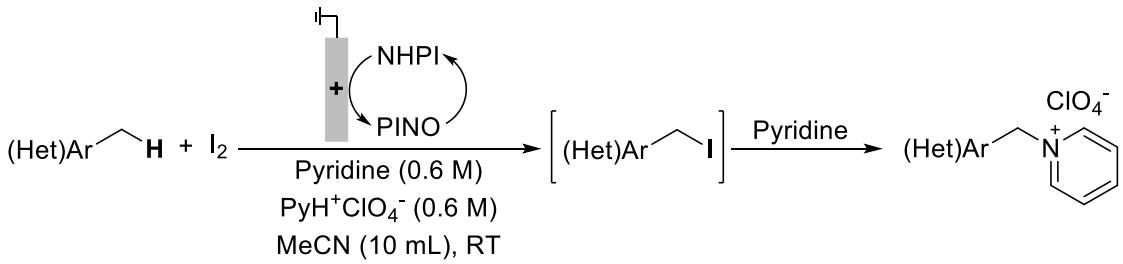

The reaction was carried out using an H-type divided cell equipped with a reticulated vitreous carbon anode (RVC, 30 PPI, 4.0 cm x 1.0 cm x 0.6 cm, ~ 3.0 cm was immersed in the solution) and a platinum wire cathode (1.0 cm, spiral wire). In the anodic chamber, methylarene (3.0 mmol), NHPI (0.45 mmol, 15 mol%), I_2 (0.06 mmol, 20 mol%), Pyridine (6.0 mmol, 0.6 M) and $PyH^+ClO_4^-$ (6.0 mmol, 0.6 M) were dissolved in CH_3CN (10.0 mL). In the cathodic chamber were placed $PyH^+ClO_4^-$ (6.0 mmol, 0.6 M) and CH_3CN (10.0 mL). Constant current electrolysis (15.0 mA, 5 mA/mmol) was carried out at room temperature with magnetic stirring. The reactions were terminated when the potentials reached to 1.20 V vs. Ag/Ag^+ (1.12 V vs Fc/Fc^+). The average reaction time was 16 hours for the substrates listed in substrate scope table. After 16 hours, the solvent from both cell compartments was removed under vacuum, then the residue was dissolved in ethyl acetate and washed with saturated $Na_2S_2O_3$ to remove the remaining iodine, followed by washing twice with aqueous $HClO_4$ (0.3 M) to remove excess pyridine/pyridinium electrolyte. The organic layer was then concentrated to afford the crude product, which was then washed with toluene twice, and dried overnight under vacuum to give the pure product.

CAUTION: The mixture of organic compounds with perchlorate is potentially explosive. For larger scale applications, the use of PF_6 salts is recommended. Crude and isolated yields of the 3-methoxybenzyl pyridinium PF_6^- salt were within 5% of those reported for the corresponding perchlorate salt, when $Py/PyH^+PF_6^-$ was used as the electrolyte.

7. Compounds Characterization

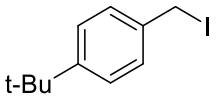

2a

The reaction was conducted following conditions A.
NMR yield: 57%
Spectra Available in the Literature: Yes[4]
^{1}H NMR (400 MHz, $CDCl_3$) δ 7.32 (s, 4H), 4.46 (s, 2H), 1.31 (s, 9H).
^{13}C NMR (100 MHz, $CDCl_3$) δ 151.0, 136.1, 128.4, 125.8, 34.6, 31.2, 6.0.

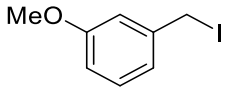

2b

The reaction was conducted following conditions A.
NMR yield: 83%; Isolated yield: 78% (194 mg, light yellow viscous liquid)
Spectra Available in the Literature: Yes[5]
^{1}H NMR (400 MHz, $CDCl_3$) δ 7.21 (t, J = 8.0 Hz, 1H), 6.97 (d, J = 8.0 Hz, 1H), 6.92 – 6.90 (m, 1H), 6.79 (dd, J = 8.0, 2.0 Hz, 1H), 4.43 (s, 2H), 3.81 (s, 3H).
^{13}C NMR (100 MHz, $CDCl_3$) δ 159.6, 140.6, 129.8, 121.0, 114.1, 113.6, 55.2, 5.6.

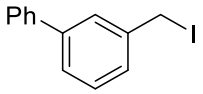

2c

The reaction was conducted following conditions A.
NMR yield: 71%
Spectra Available in the Literature: No
^{1}H NMR (400 MHz, $CDCl_3$) δ 7.60 – 7.51 (m, 3H), 7.46 – 7.37 (m, 3H), 7.36 – 7.27 (m, 3H), 4.46 (s, 2H).
^{13}C NMR (100 MHz, $CDCl_3$) δ 141.8, 140.5, 139.7, 129.2, 128.8, 127.54, 127.51, 127.49, 127.1, 126.7, 5.6.
HRMS (**ESI**) Calculated for C13H12I ($[M+H]^+$): 294.9978, measured: 294.9975.

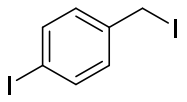

2d

The reaction was conducted following conditions A.
NMR yield: 69%
Spectra Available in the Literature: Yes[6]
^{1}H NMR (400 MHz, $CDCl_3$) δ 7.62 (d, J = 8.4 Hz, 2H), 7.12 (d, J = 8.4 Hz, 2H), 4.38 (s, 2H).
^{13}C NMR (100 MHz, $CDCl_3$) δ 138.9, 137.9, 130.5, 93.3, 4.3.

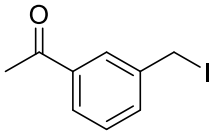

2e

The reaction was conducted following conditions B.
NMR yield: 57%
When the reaction was conducted using conditions A, the NMR yield was 51%.
Spectra Available in the Literature: Yes[7]
^{1}H NMR (400 MHz, $CDCl_3$) δ 7.95 (s, 1H), 7.82 (d, *J* = 7.8 Hz, 1H), 7.57 (d, *J* = 7.7 Hz, 1H), 7.39 (t, *J* = 7.7 Hz, 1H), 4.48 (s, 2H), 2.59 (s, 3H).
^{13}C NMR (100 MHz, $CDCl_3$) δ 197.4, 140.0, 137.5, 133.3, 129.1, 128.2, 127.7, 26.6, 4.2.

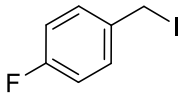

2f

The reaction was conducted following conditions B.
NMR yield: 68%; Isolated yield: 62% (147 mg, light yellow solid); the NMR yield was 56% under conditions A.
Spectra Available in the Literature: Yes[8]
^{1}H NMR (400 MHz, $CDCl_3$) δ 7.40 – 7.31 (m, 2H), 7.04 – 6.93 (m, 2H), 4.44 (s, 2H).
^{13}C NMR (100 MHz, $CDCl_3$) δ 162.1 (d, *J* = 246.4 Hz), 135.2 (d, *J* = 3.4 Hz), 130.4 (d, *J* = 8.6 Hz), 115.8 (d, *J* = 21.5 Hz), 4.5.

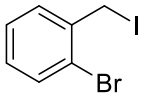

2g

The reaction was conducted following conditions B.
NMR yield: 69%; isolated yield 68%, (201 mg, brown oil); the NMR yield was 58% under conditions A.
Spectra Available in the Literature: Yes[7]
^{1}H NMR (400 MHz, $CDCl_3$) δ 7.51 (dd, *J* = 8.0, 1.2 Hz, 1H), 7.42 (dd, *J* = 7.6, 1.6 Hz, 1H), 7.24 (td, *J* = 7.6, 1.2 Hz, 1H), 7.10 (td, *J* = 8.0, 1.6 Hz, 1H), 4.53 (s, 2H).
^{13}C NMR (100 MHz, $CDCl_3$) δ 138.3, 133.5, 130.6, 129.5, 128.0, 124.1, 5.8.

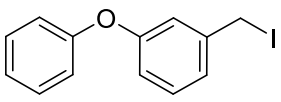

2h

The reaction was conducted following conditions B.
NMR Yield: 70%; Isolated yield 67% (207 mg, light red oil); the NMR yield was 56% under conditions A.

Spectra Available in the Literature: No

^{1}H NMR (400 MHz, $CDCl_3$) δ 7.39 – 7.31 (m, 2H), 7.24 (t, *J* = 8.0 Hz, 1H), 7.16 – 7.07 (m, 2H), 7.05 – 6.96 (m, 3H), 6.86 (dd, *J* = 8.4, 2.0 Hz, 1H), 4.39 (s, 2H).

^{13}C NMR (100 MHz, $CDCl_3$) δ 157.5, 156.7, 141.1, 130.1, 129.8, 123.5, 123.4, 119.0, 118.8, 118.1, 4.8.

HRMS (**ESI**) Calculated for C13H12OI ($[M+H]^+$): 310.9927, measured: 310.9921.

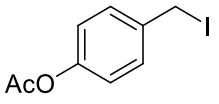

2i

The reaction was conducted following conditions A.

NMR yield: 40%; isolated yield 36% (99 mg white solid)

Spectra Available in the Literature: Yes[7]

^{1}H NMR (500 MHz, $CDCl_3$) δ 7.39 (d, *J* = 8.4 Hz, 2H), 7.02 (d, *J* = 8.4 Hz, 2H), 4.44 (s, 2H), 2.29 (s, 3H)

^{13}C NMR (125 MHz, $CDCl_3$) δ 168.2, 150.0, 135.8, 128.9, 120.9, 20.1, 3.5.

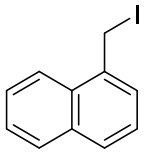

2j

The reaction was conducted following conditions A.

NMR yield: 77%

Spectra Available in the Literature: No.

This compound decomposed during MS characterization.

^{1}H NMR (400 MHz, $CDCl_3$) δ 7.81 – 7.70 (m, 4H), 7.46 – 7.40 (m, 3H), 4.58 (s, 2H).

^{13}C NMR (100 MHz, $CDCl_3$) δ 136.5, 133.2, 132.7, 128.7, 127.8, 127.7, 127.0, 126.9, 126.4, 126.3, 6.5.

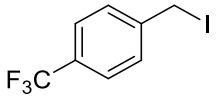

2k

The reaction was conducted following conditions A.

NMR yield: 39%

Spectra Available in the Literature: Yes[9]

^{1}H NMR (400 MHz, $CDCl_3$) δ 7.56 (d, *J* = 8.4 Hz, 1H), 7.48 (d, *J* = 8.4 Hz, 1H), 4.46 (s, 1H).

^{13}C NMR (100 MHz, $CDCl_3$) δ 143.3 (q, *J* = 1.3 Hz), 129.9 (q, *J* = 32.6 Hz), 129.0, 125.8 (q, *J* = 3.8 Hz), 123.9 (q, *J* = 272.1 Hz), 3.2.

^{19}F NMR (377 MHz, $CDCl_3$) δ -62.68 (s).

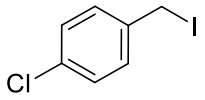

2l

The reaction was conducted following conditions B.
NMR yield: 67%; the NMR yield was 61% under conditions A.
Spectra Available in the Literature: Yes[9]
^{1}H NMR (400 MHz, $CDCl_3$) δ 7.30 (d, *J* = 8.4 Hz, 2H), 7.25 (d, *J* = 8.4 Hz, 2H), 4.41 (s, 2H).
^{13}C NMR (100 MHz, $CDCl_3$) δ 137.8, 133.6, 130.0, 129.0, 4.2.

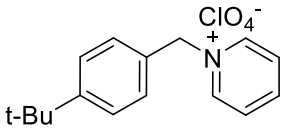

3

The reaction was conducted following the general procedure for benzyl pyridinium formation.
NMR yield: 89%; isolated yield 81% (792 mg, light yellow solid)
Spectra Available in the Literature: No
^{1}H NMR (400 MHz, CD_3CN) δ 8.78 (d, *J* = 5.2 Hz, 2H), 8.51 (t, *J* = 7.2 Hz, 1H), 8.03 (t, *J* = 7.2 Hz, 2H), 7.50 (d, *J* = 7.6 Hz, 2H), 7.39 (d, *J* = 7.6 Hz, 2H), 5.70 (s, 2H), 1.28 (s, 9H).
^{13}C NMR (100 MHz, CD_3CN) δ 154.1, 147.1, 145.4, 131.1, 129.9, 129.6, 127.4, 65.1, 35.4, 31.3.
HRMS (**ESI**) Calculated for $C16H20N^+$ ($M\text{-}ClO_4^-$): 226.1590, measured: 226.1592.

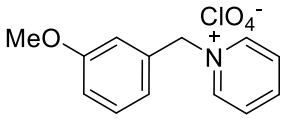

4

The reaction was conducted following the general procedure for benzyl pyridinium formation.
NMR yield: 93%; isolated yield 83% (747 mg, light yellow solid)
Spectra Available in the Literature: No
^{1}H NMR (400 MHz, CD_3CN) δ 8.81 (d, *J* = 5.6 Hz, 2H), 8.54 (t, *J* = 7.6 Hz, 1H), 8.06 (t, *J* = 6.4 Hz, 2H), 7.41 (t, *J* = 7.6 Hz, 1H), 7.10 – 6.99 (m, 3H), 5.71 (s, 2H), 3.82 (s, 3H).
^{13}C NMR (100 MHz, CD_3CN) δ 161.4, 147.3, 145.6, 135.3, 131.8, 129.6, 122.3, 116.4, 115.8, 65.4, 56.2.
HRMS (**ESI**) Calculated for $C13H14NO^+$ ($M\text{-}ClO_4^-$): 200.1070, measured: 200.1069.

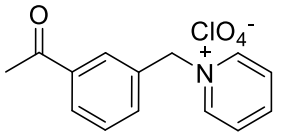

5

The reaction was conducted following the general procedure for benzyl pyridinium formation.
NMR yield: 62%; isolated yield 53% (496 mg, light yellow solid)
Spectra Available in the Literature: No

^{1}H NMR (400 MHz, CD_3CN) δ 8.84 (d, *J* = 5.6 Hz, 2H), 8.52 (t, *J* = 7.6 Hz, 1H), 8.10 (s, 1H), 8.05 – 7.97 (m, 3H), 7.71 (d, *J* = 7.6 Hz, 1H), 7.56 (t, *J* = 7.6 Hz, 1H), 5.81 (s, 2H), 2.58 (s, 3H).
^{13}C NMR (100 MHz, CD_3CN) δ 200.5, 146.8, 145.0, 138.2, 134.6, 133.9, 130.4, 130.1, 130.0, 129.1, 64.3, 26.9.
HRMS (**ESI**) Calculated for $C14H14NO^+$ ($M\text{-}ClO_4^-$): 212.1070, measured: 212.1069.

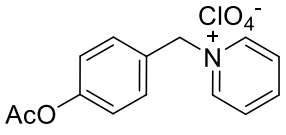

6

The reaction was conducted following the general procedure for benzyl pyridinium formation.
NMR yield: 40%
Spectra Available in the Literature: No
The product decomposed during purification. Therefore, the crude NMR spectrum is provided below.
HRMS (**ESI**) Calculated for $C14H14NO2^+$ ($M\text{-}ClO_4^-$): 228.1019, measured: 228.1020.

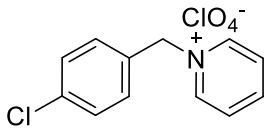

7

The reaction was conducted following the general procedure for benzyl pyridinium formation.
NMR yield: 84%
Spectra Available in the Literature: Yes[10]
^{1}H NMR (400 MHz, CD_3CN) δ 8.79 (d, *J* = 5.6 Hz, 2H), 8.57 – 8.47 (m, 1H), 8.07 – 7.98 (m, 2H), 7.48 – 7.39 (m, 4H), 5.73 (s, 2H).
^{13}C NMR (100 MHz, CD_3CN) δ 146.8, 144.9, 135.6, 132.3, 131.6, 129.9, 129.1, 63.9.

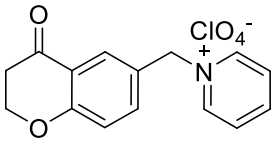

8

The reaction was conducted following the general procedure for benzyl pyridinium formation.
NMR yield: 90%; isolated yield 74% (251 mg, light yellow solid)
Spectra Available in the Literature: No
^{1}H NMR (400 MHz, CD_3CN) δ 8.75 (d, *J* = 5.6 Hz, 2H), 8.50 (t, *J* = 7.6 Hz, 1H), 8.01 (t, *J* = 7.2 Hz, 2H), 7.95 (d, *J* = 2.4 Hz, 1H), 7.59 (dd, *J* = 8.6, 2.4 Hz, 1H), 7.08 (d, *J* = 8.6 Hz, 1H), 5.68 (s, 2H), 4.56 (t, *J* = 6.4 Hz, 2H), 2.78 (t, *J* = 6.4 Hz, 2H).
^{13}C NMR (100 MHz, CD_3CN) δ 192.1, 163.7, 147.2, 145.3, 137.6, 129.6, 129.2, 126.5, 122.6, 120.3, 68.3, 64.6, 38.0.
HRMS (**ESI**) Calculated for $C15H14NO2^+$ ($M\text{-}ClO_4^-$): 240.1019, measured: 240.1021.

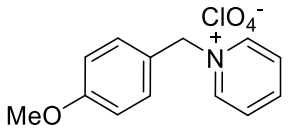

9

The reaction was conducted following the general procedure for benzyl pyridinium formation.
NMR yield: 86%
Spectra Available in the Literature: Yes[11]
The product decomposed during purification. Therefore, the crude NMR spectrum is provided in the collection of spectra below.

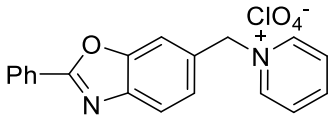

10

The reaction was conducted following the general procedure for benzyl pyridinium formation.
NMR yield: 56%
Spectra Available in the Literature: No
The product decomposed during purification. Therefore, the crude NMR spectrum is provided in the collection of spectra below.
HRMS (**ESI**) Calculated for $C19H15N2O^+$ ($M\text{-}ClO_4^-$): 287.1179, measured: 287.1180.

8. Further Transformations of Benzyl Iodides

1) C-N bond formation

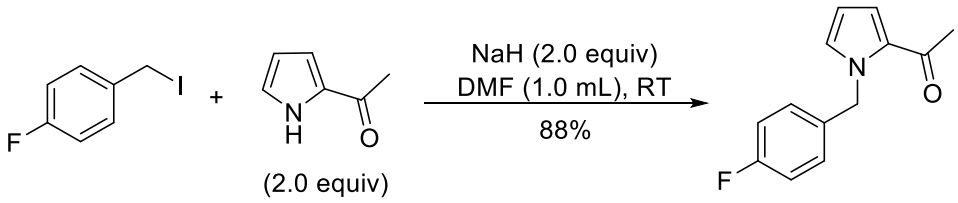

(2-Pyrrolyl)ethenone (0.24 mmol, 2.0 equiv.) and NaH (0.24 mmol, 2.0 equiv.) were added into DMF (0.5 mL), to which was added the solution of **2f** (0.12 mmol in 0.5 mL DMF) dropwise. The mixture was stirred at room temperature for 3 h, after that the reaction mixture was extracted with EtOAc and water. The organic layers were combined, dried over Na_2SO_4 and concentrated, the residue was purified by column chromatography on silica gel with a gradient eluent of pentane and ethyl acetate to give **11** (23 mg, light yellow oil). The spectrum was consistent with the literature data.[12]

^{1}H NMR (400 MHz, $CDCl_3$) δ 7.14 – 7.06 (m, 2H), 7.01 (dd, *J* = 4.0, 1.6 Hz, 1H), 6.99 – 6.95 (m, 2H), 6.91 (dd, *J* = 2.4, 1.6 Hz, 1H), 6.20 (dd, *J* = 4.0, 2.4 Hz, 1H), 5.53 (s, 2H), 2.41 (s, 3H).

^{13}C NMR (100 MHz, $CDCl_3$) δ 188.4, 162.0 (d, *J* = 245.6 Hz), 134.0 (d, *J* = 3.2 Hz), 130.2, 130.1, 128.7 (d, *J* = 8.1 Hz), 120.5, 115.4 (d, *J* = 21.5 Hz), 108.6, 51.8, 27.2.

2) C-O bond formation

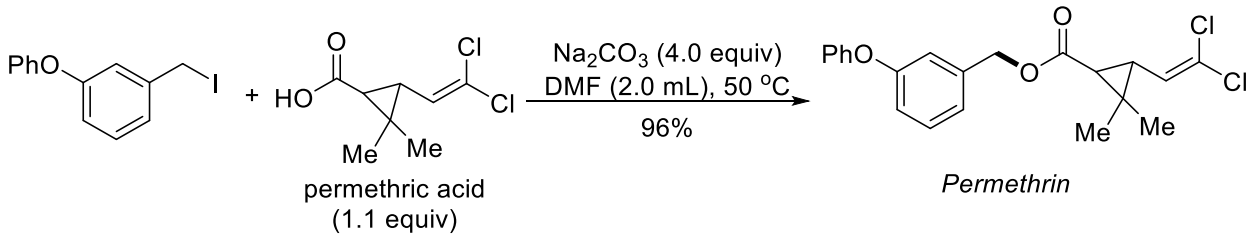

2h (0.2 mmol) and Permethric acid (0.22 mmol, 1.1 equiv.) were dissolved in DMF (2.0 mL), followed by addition of Na_2CO_3 (4.0 equiv.). The mixture was stirred at 50 ^{o}C for 6 h, after that the reaction mixture was cooled to room temperature and extracted with EtOAc and water. The organic layers were combined, dried over Na_2SO_4 and concentrated, the residue was purified by column chromatography on silica gel with a gradient eluent of pentane and ethyl acetate to give **12** (75 mg, viscous oil). The spectrum was consistent with the literature data.[13]

cis-permethrin:

^{1}H NMR (400 MHz, $CDCl_3$) δ 7.37 – 6.29 (m, 3H), 7.13 (t, *J* = 7.6 Hz, 1H), 7.09 (d, *J* = 7.6 Hz, 1H), 7.06 – 6.99 (m, 3H), 6.97 (dd, *J* = 8.0, 1.6 Hz, 1H), 6.27 (d, *J* = 9.2 Hz, 1H), 5.10 (d, *J* = 12.4 Hz, 1H), 5.06 (d, *J* = 12.4 Hz, 1H), 2.05 (t, *J* = 8.4 Hz, 1H), 1.90 (d, *J* = 8.4 Hz, 1H), 1.25 (s, 3H),

1.25 (s, 3H).
^{13}C NMR (100 MHz, $CDCl_3$) δ 170.3, 157.5, 156.9, 137.9, 129.9, 129.8, 124.8, 123.5, 122.7, 120.7, 119.0, 118.4, 118.2, 65.7, 32.7, 31.8, 28.3, 27.7, 14.9.
trans-permethrin:
^{1}H NMR (400 MHz, $CDCl_3$) δ 7.40 – 7.31 (m, 3H), 7.13 (t, *J* = 7.6 Hz, 1H), 7.09 (d, *J* = 7.6 Hz, 1H), 7.05 – 6.99 (m, 3H), 6.96 (dd, *J* = 8.4, 1.6 Hz, 1H), 5.61 (d, *J* = 8.4 Hz, 1H), 5.12 (d, *J* = 13.2 Hz, 1H), 5.09 (d, *J* = 13.2 Hz, 2H), 2.26 (dd, *J* = 8.4, 5.2 Hz, 1H), 1.66 (d, *J* = 5.2 Hz, 1H), 1.28 (s, 3H), 1.19 (s, 3H).
^{13}C NMR (100 MHz, $CDCl_3$) δ 170.9, 157.5, 156.9, 137.9, 129.9, 129.8, 126.9, 123.5, 122.7, 122.1, 119.0, 118.4, 118.2, 66.0, 34.6, 33.0, 29.1, 22.6, 20.0.

3) C-C bond formation

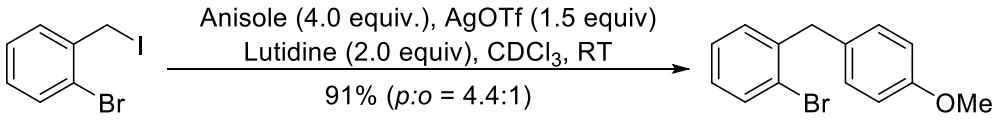

Anisole (0.4 mmol, 4.0 equiv.), Lutidine (0.2 mmol, 2.0 equiv.) and AgOTf (0.15 mmol, 1.5 equiv.) were added into $CDCl_3$ (0.5 mL). To this suspension was added dropwise the solution of **2g** in $CDCl_3$ (0.5 mL, 0.2 M) at room temperature, during which yellow solid was generated. The mixture was stirred for 1hr, then filtered through a short pad of celite and washed with ethyl acetate (10 mL). After evaporation, the residue was purified by column chromatography on silica gel with a gradient eluent of pentane and ethyl acetate to give **13** (25 mg, *p:o* = 4.4:1, colorless oil). The spectrum was consistent with the literature data.[14]
^{1}H NMR (400 MHz, $CDCl_3$) δ 7.56 (dd, *J* = 8.0, 1.2 Hz, 1H), 7.22 (td, *J* = 7.6, 1.2 Hz, 1H), 7.14 – 7.04 (m, 4H), 6.84 (d, *J* = 8.4 Hz, 2H), 4.05 (s, 2H), 3.79 (s, 3H).
^{13}C NMR (100 MHz, $CDCl_3$) δ 158.0, 140.8, 132.8, 131.5, 130.9, 130.0, 127.8, 127.4, 124.8, 113.9, 55.2, 40.9.

9. NMR Spectra of Compounds.

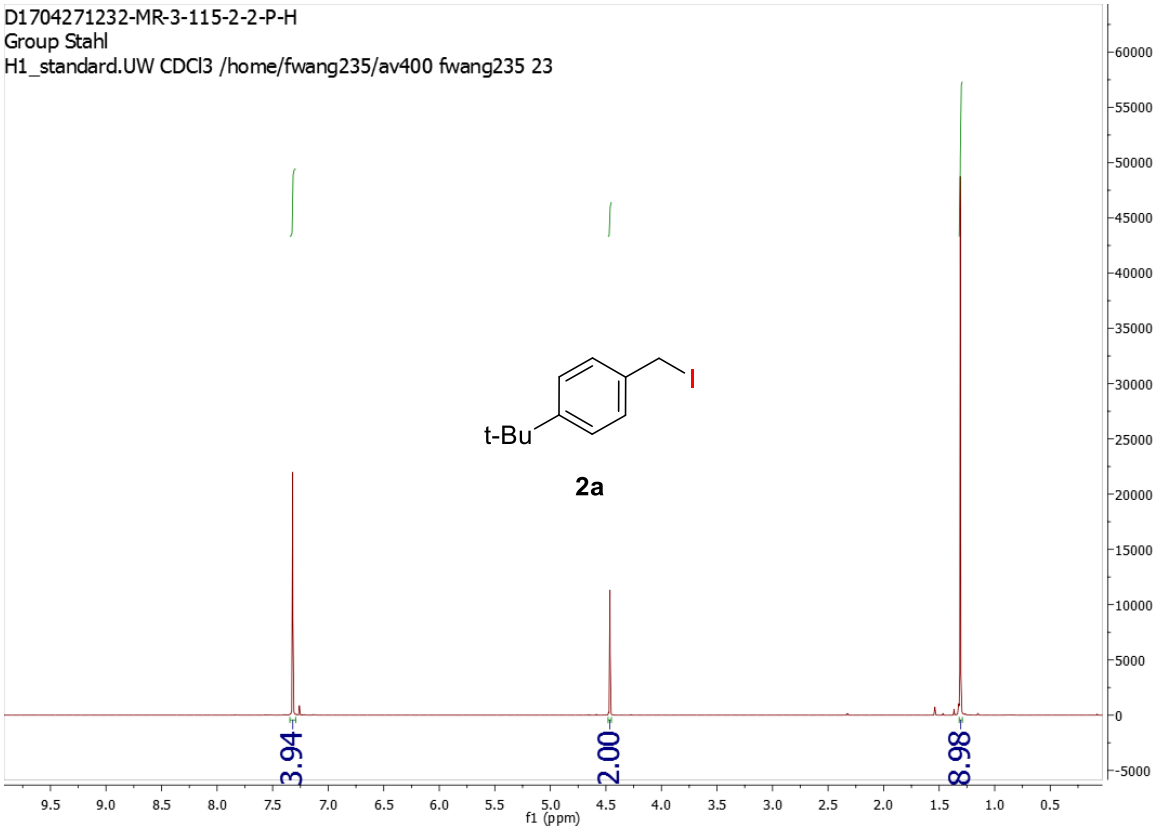

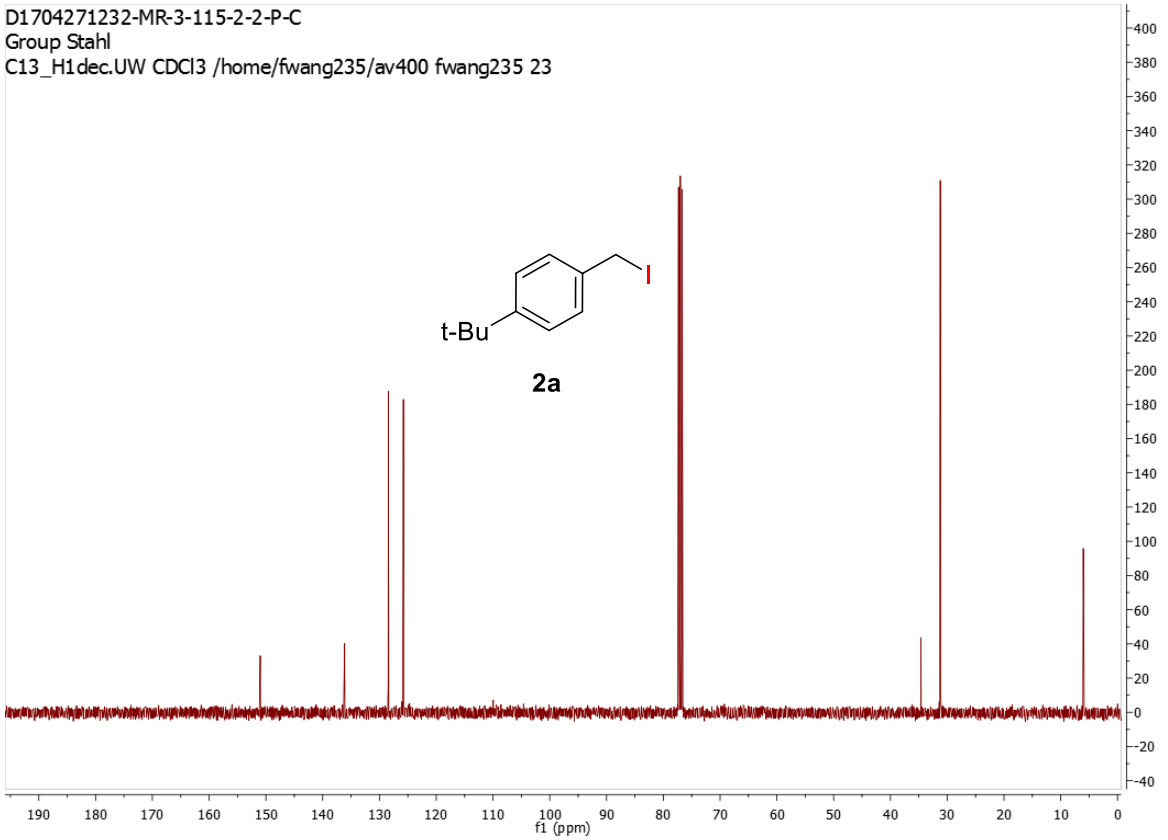

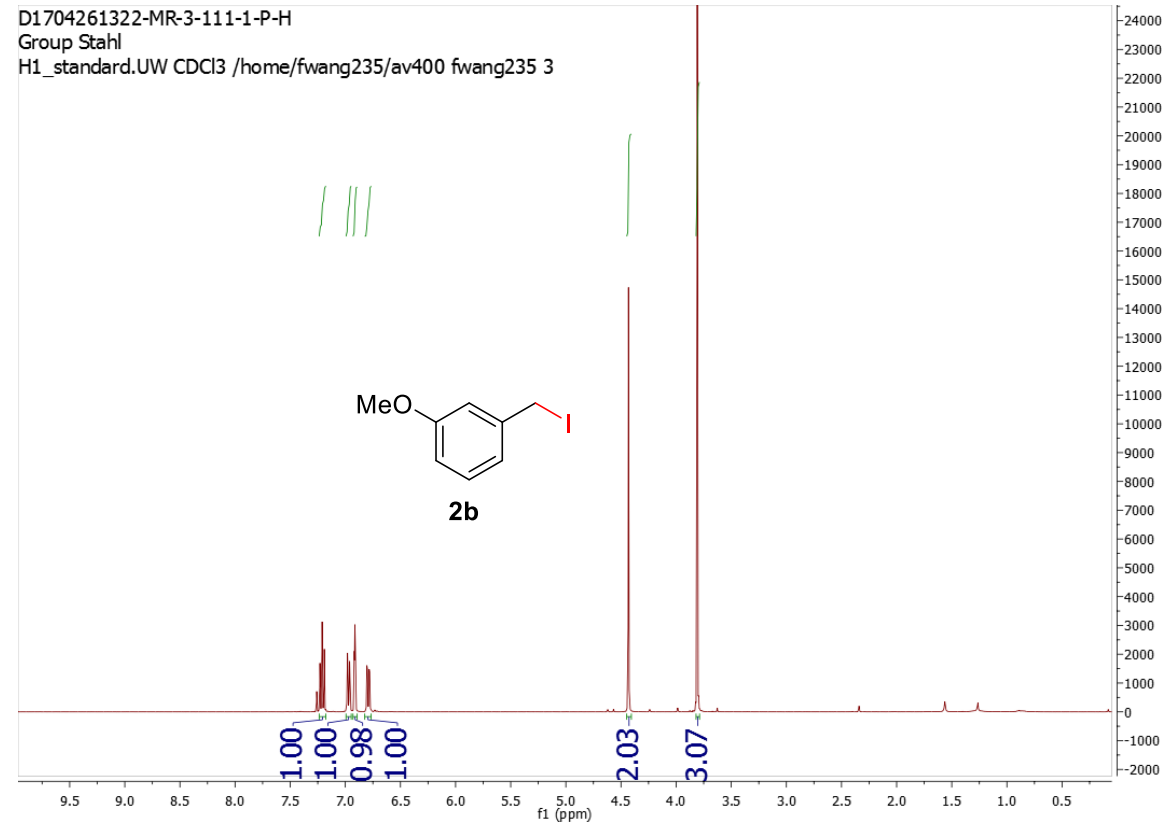
D1704261322-MR-3-111-1-P-H
Group Stahl
H1_standard.UW CDCl3 /home/fwang235/av400 fwang235 3
MeO
I
2b
1.00
1.00
0.98
1.00
2.03
3.07
f1 (ppm)

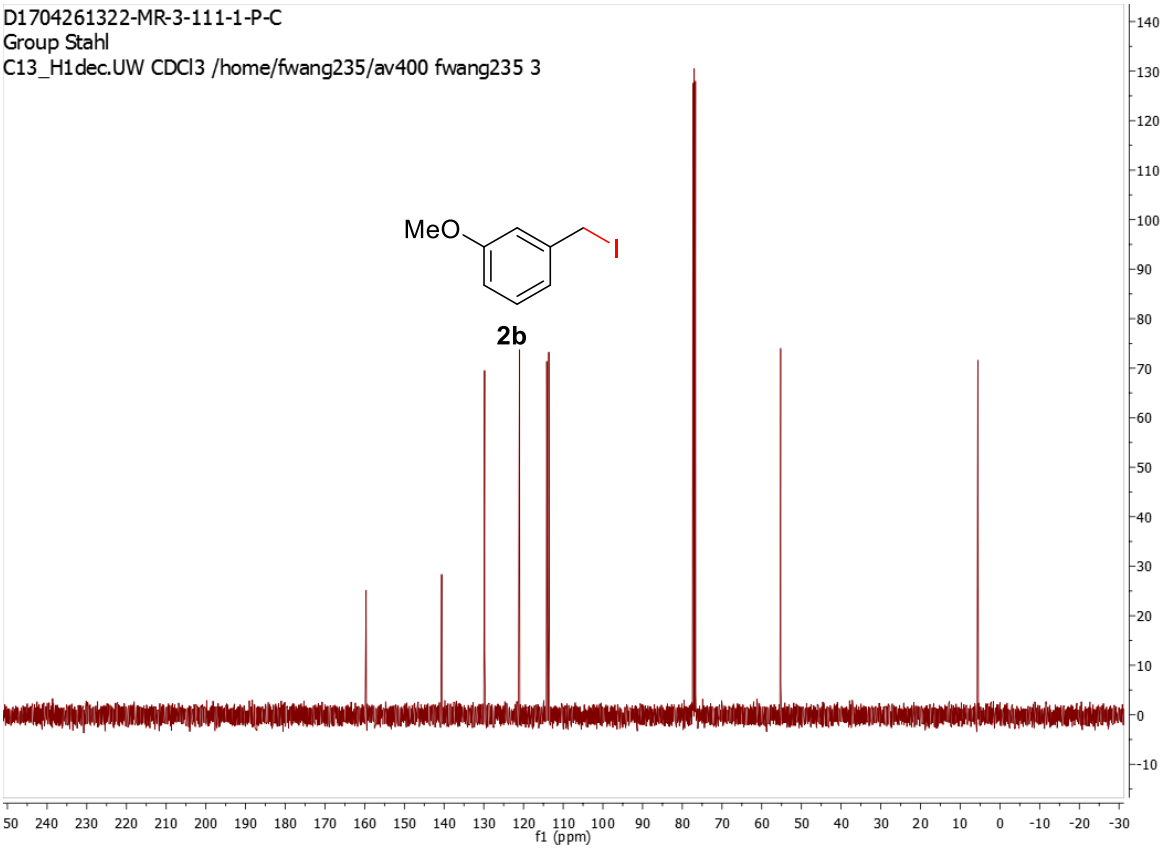
D1704261322-MR-3-111-1-P-C
Group Stahl
C13_H1dec.UW CDCl3 /home/fwang235/av400 fwang235 3
MeO
I
2b
f1 (ppm)

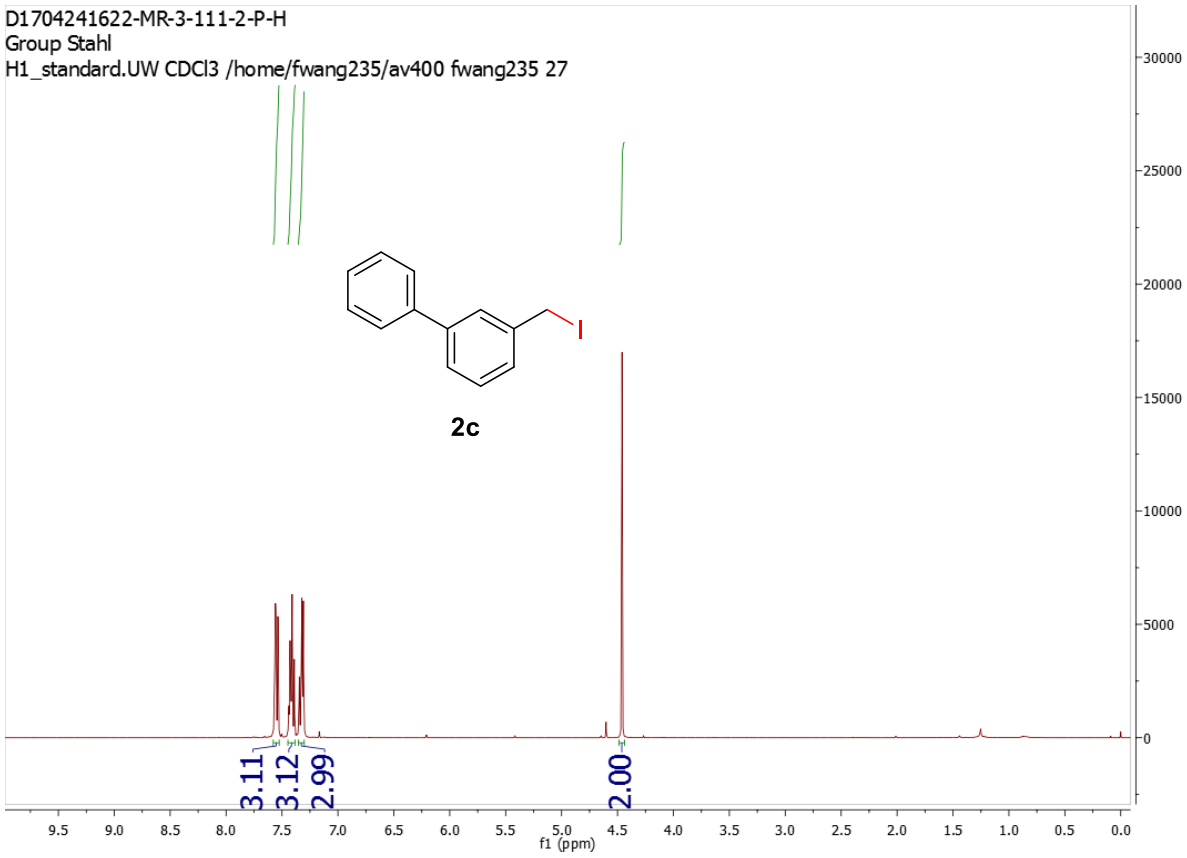
D1704241622-MR-3-111-2-P-H
Group Stahl
H1_standard.UW CDCl3 /home/fwang235/av400 fwang235 27
2c
3.11
3.12
2.99
2.00
f1 (ppm)

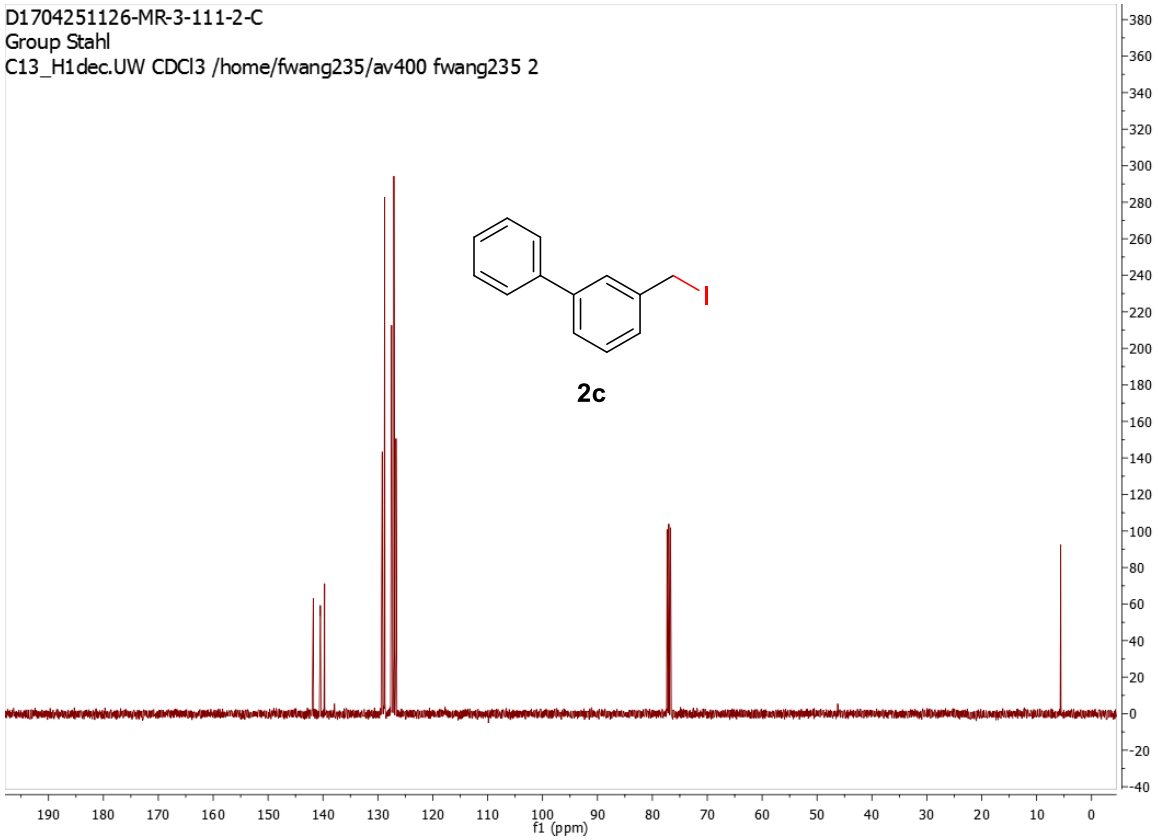
D1704251126-MR-3-111-2-C
Group Stahl
C13_H1dec.UW CDCl3 /home/fwang235/av400 fwang235 2
2c
f1 (ppm)

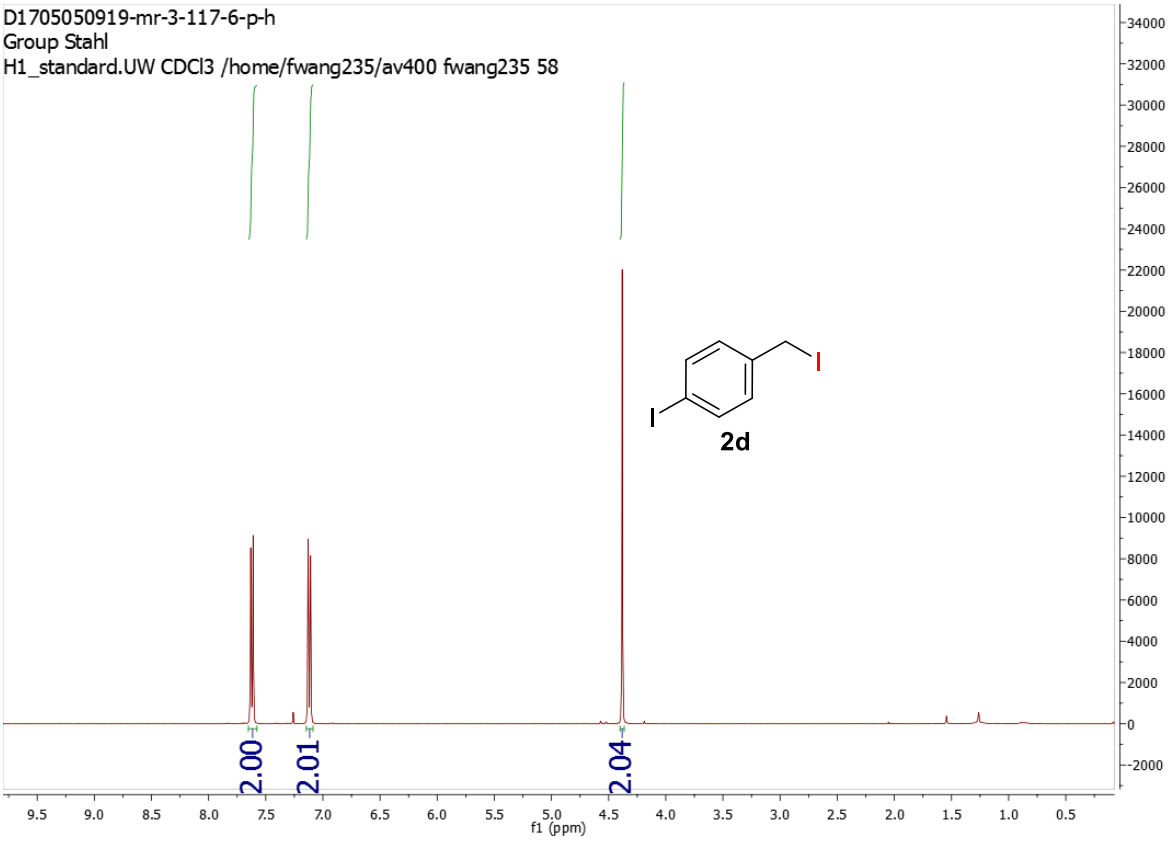
D1705050919-mr-3-117-6-p-h
Group Stahl
H1_standard.UW CDCl3 /home/fwang235/av400 fwang235 58
2d
2.00
2.01
2.04
f1 (ppm)

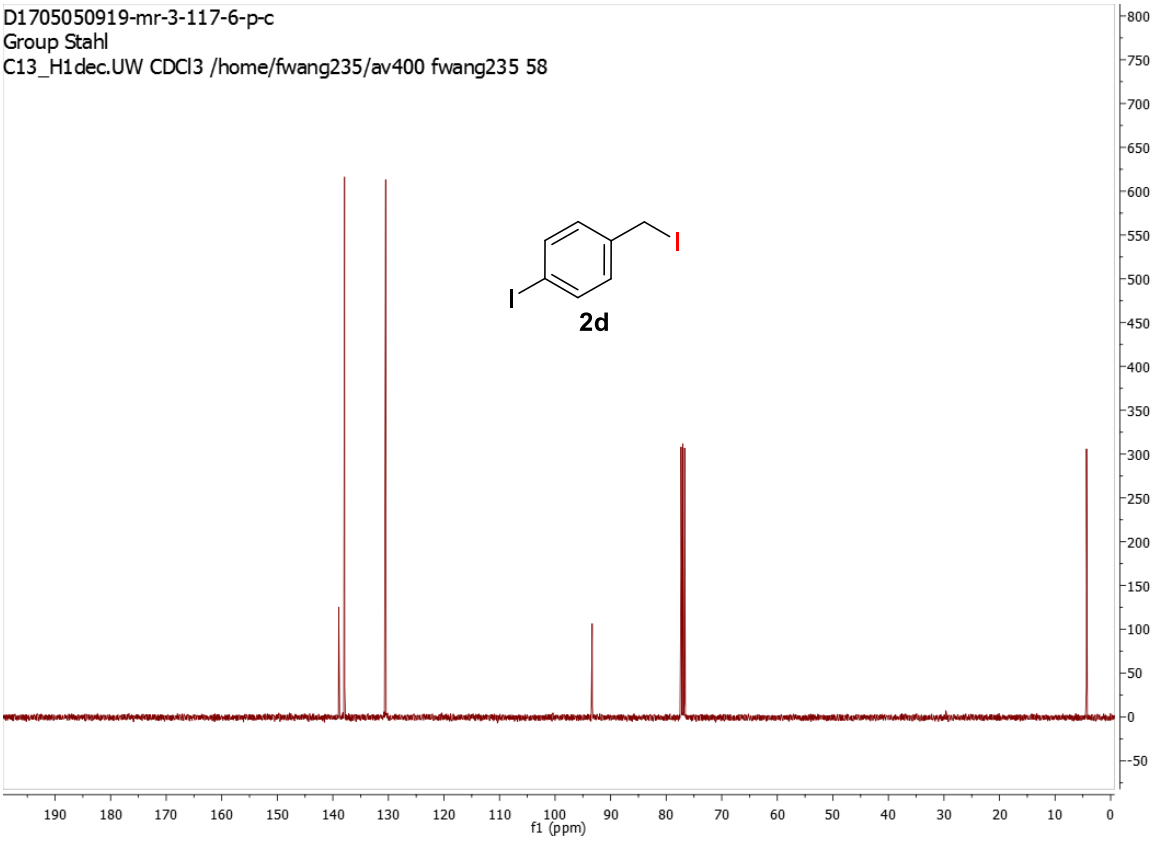
D1705050919-mr-3-117-6-p-c
Group Stahl
C13_H1dec.UW CDCl3 /home/fwang235/av400 fwang235 58
2d
f1 (ppm)

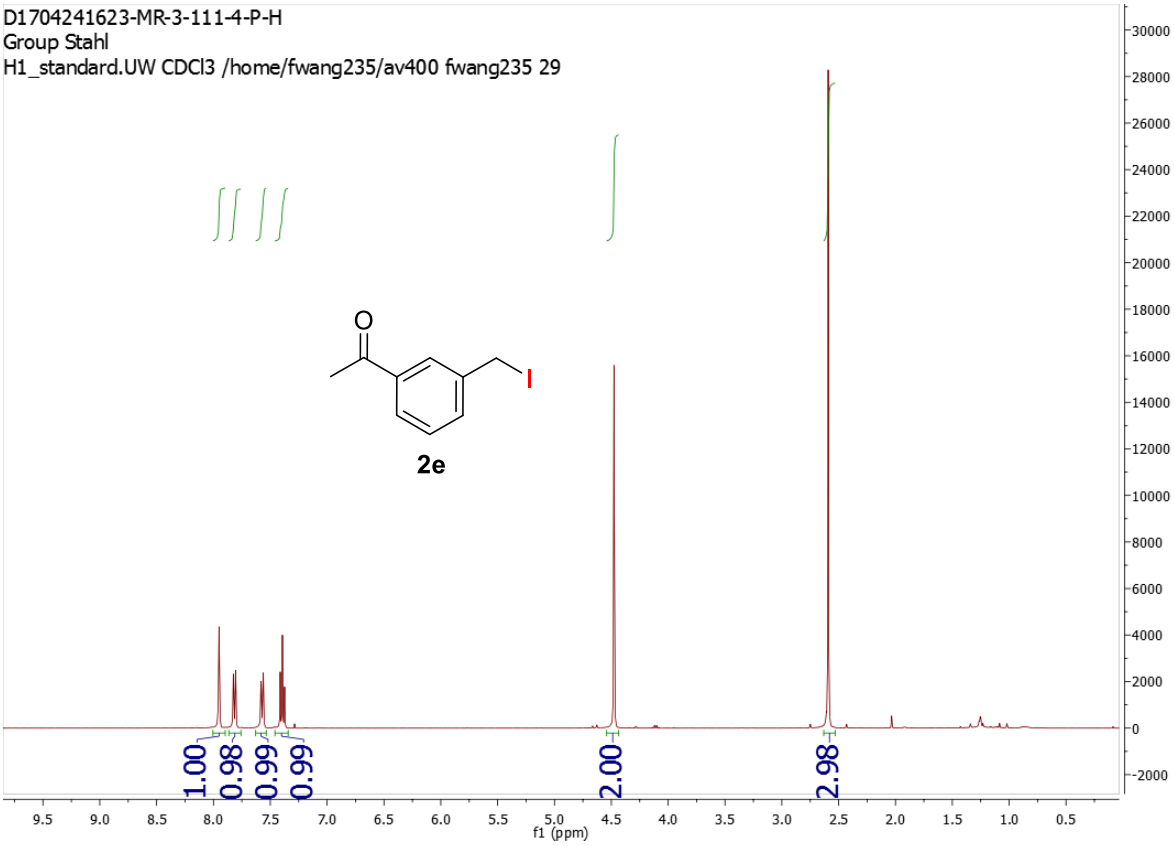
D1704241623-MR-3-111-4-P-H
Group Stahl
H1_standard.UW CDCl3 /home/fwang235/av400 fwang235 29
O
I
2e
1.00
0.98
0.99
0.99
2.00
2.98
f1 (ppm)

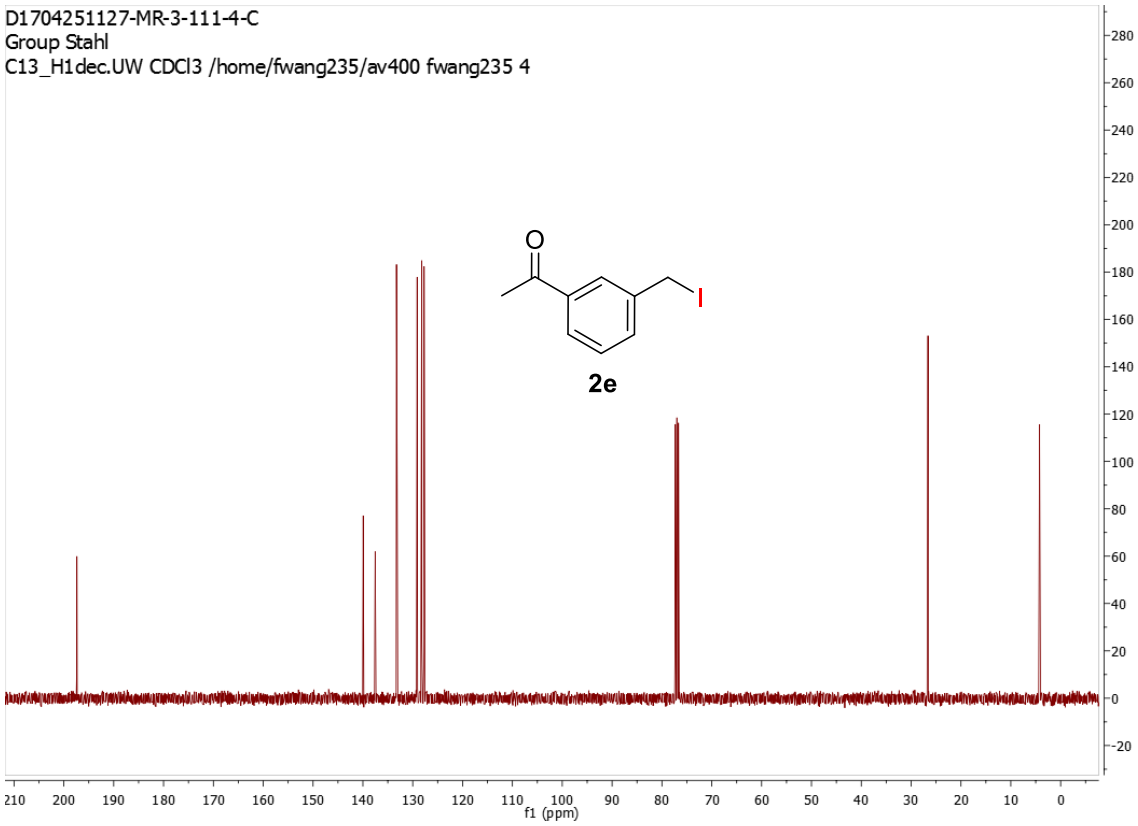
D1704251127-MR-3-111-4-C
Group Stahl
C13_H1dec.UW CDCl3 /home/fwang235/av400 fwang235 4
O
I
2e
f1 (ppm)

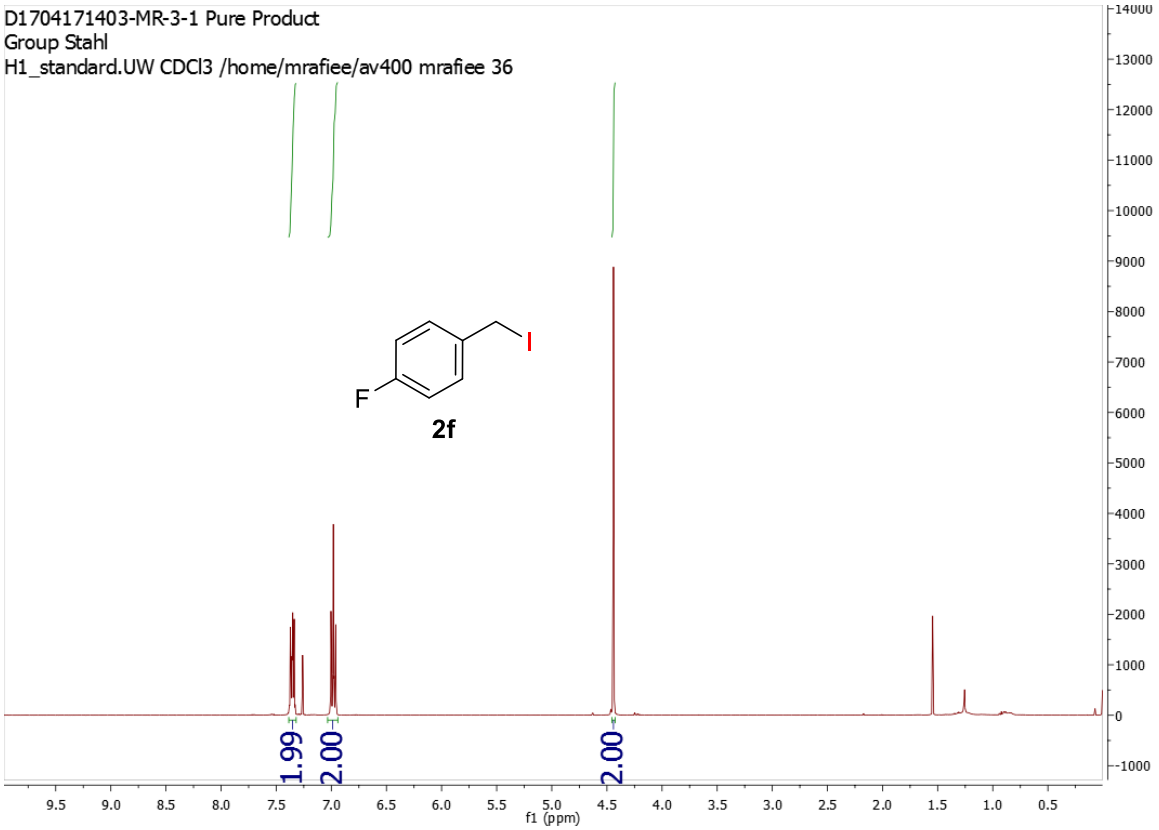
D1704171403-MR-3-1 Pure Product
Group Stahl
H1_standard.UW CDCl3 /home/mrafiee/av400 mrafiee 36
F
I
2f
1.99
2.00
2.00
f1 (ppm)

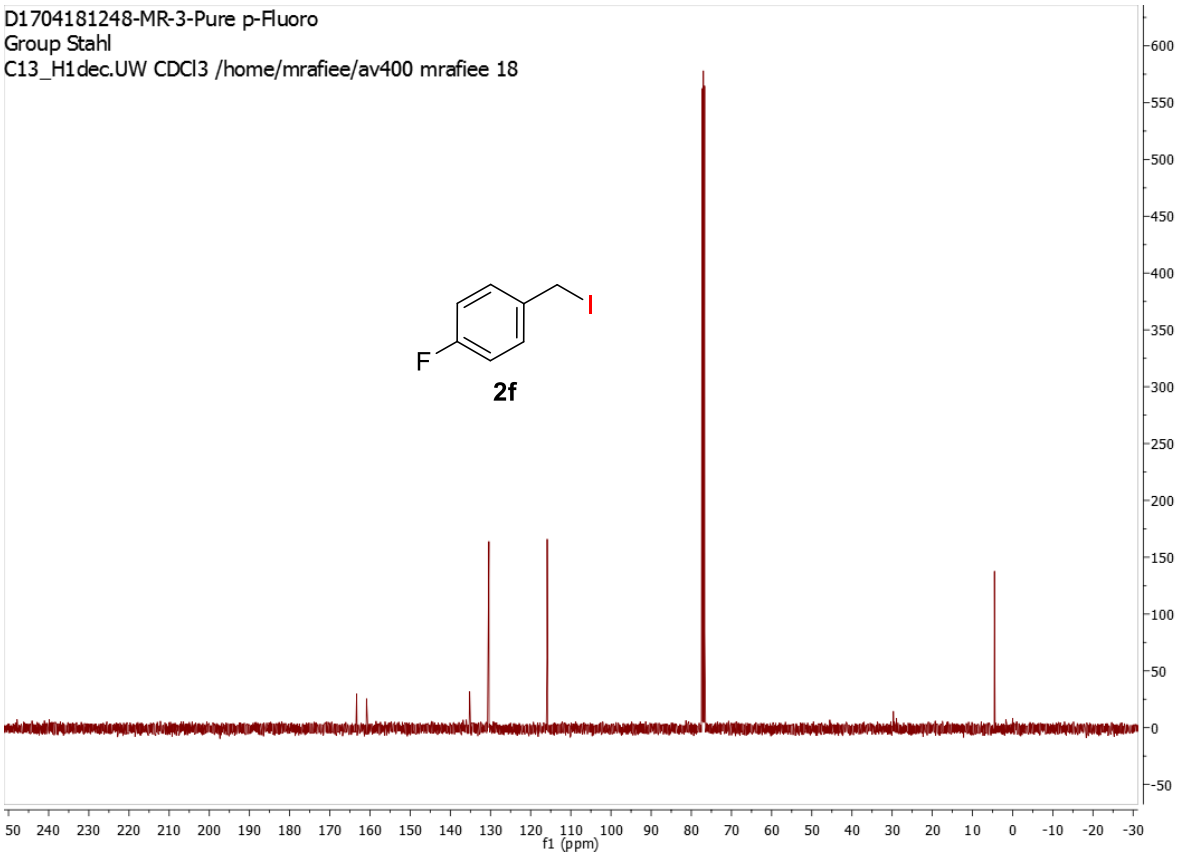
D1704181248-MR-3-Pure p-Fluoro
Group Stahl
C13_H1dec.UW CDCl3 /home/mrafiee/av400 mrafiee 18
F
I
2f
f1 (ppm)

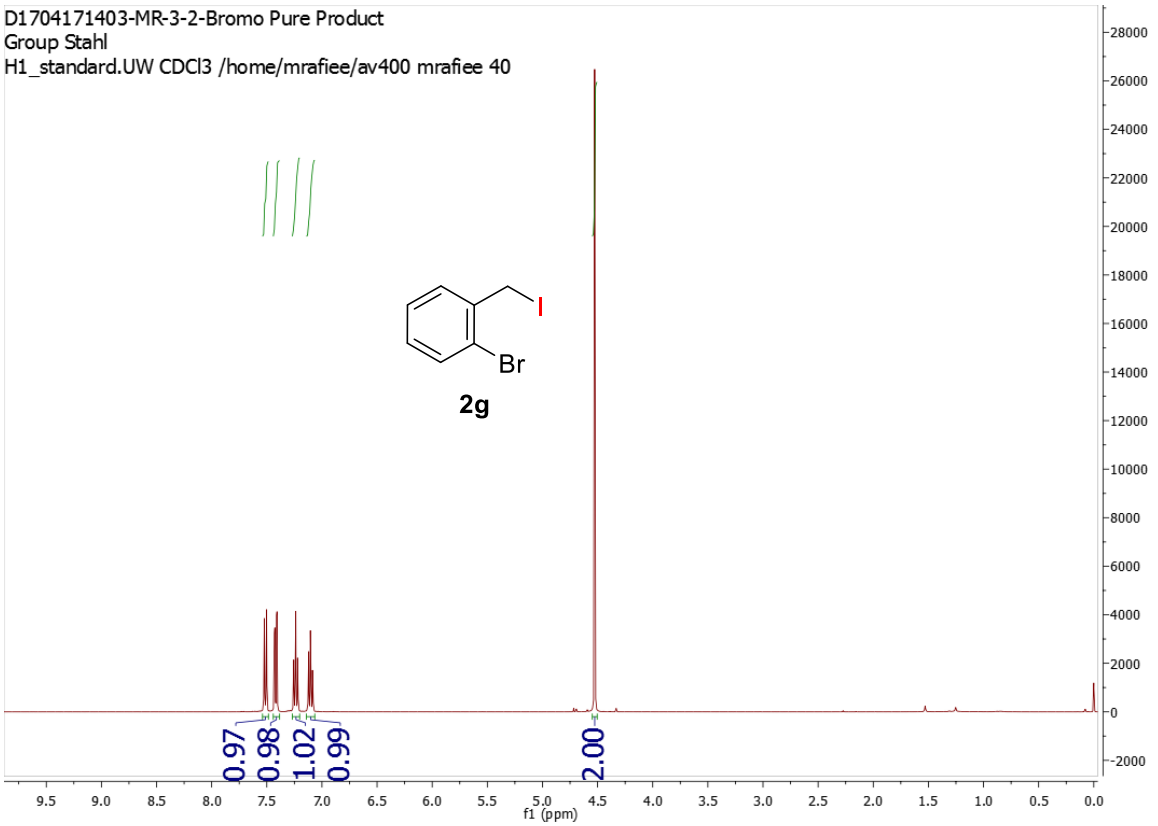
D1704171403-MR-3-2-Bromo Pure Product
Group Stahl
H1_standard.UW CDCl3 /home/mrafiee/av400 mrafiee 40
Br
2g
0.97
0.98
1.02
0.99
2.00
f1 (ppm)

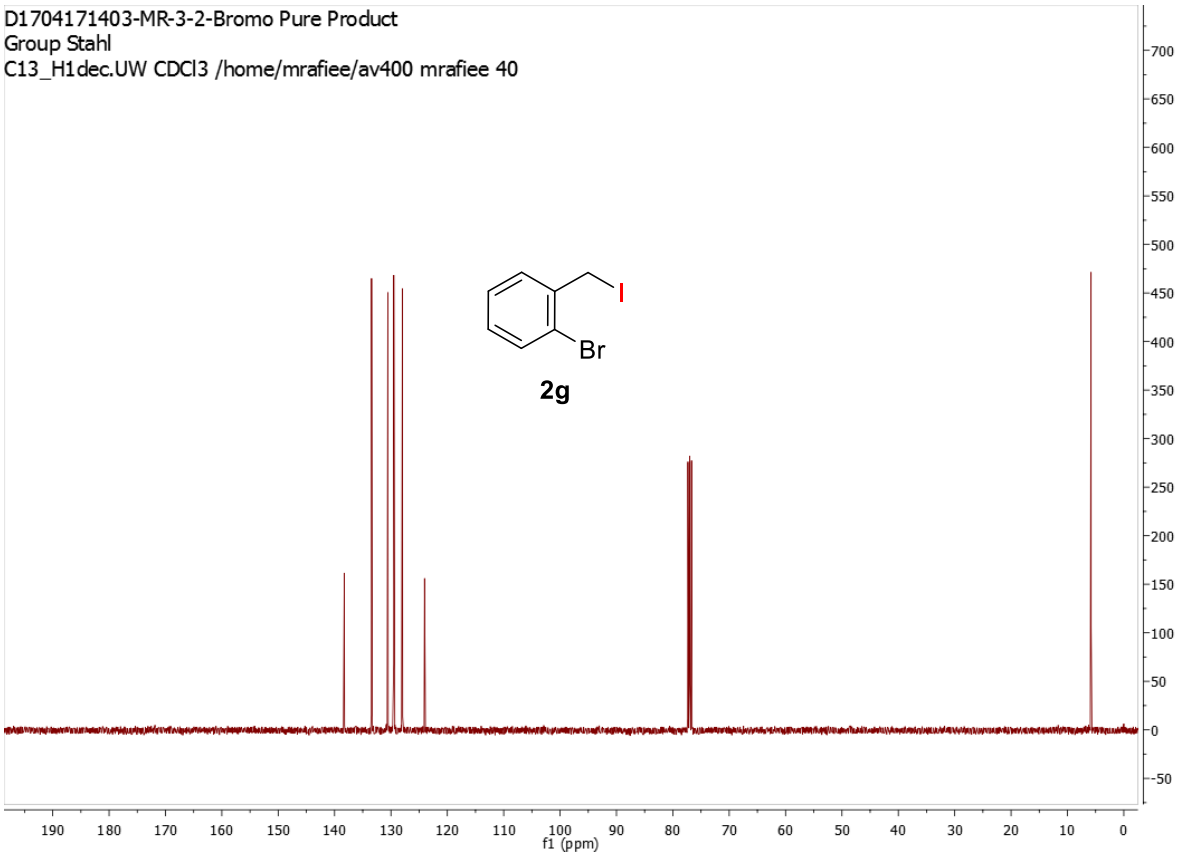
D1704171403-MR-3-2-Bromo Pure Product
Group Stahl
C13_H1dec.UW CDCl3 /home/mrafiee/av400 mrafiee 40
Br
2g
f1 (ppm)

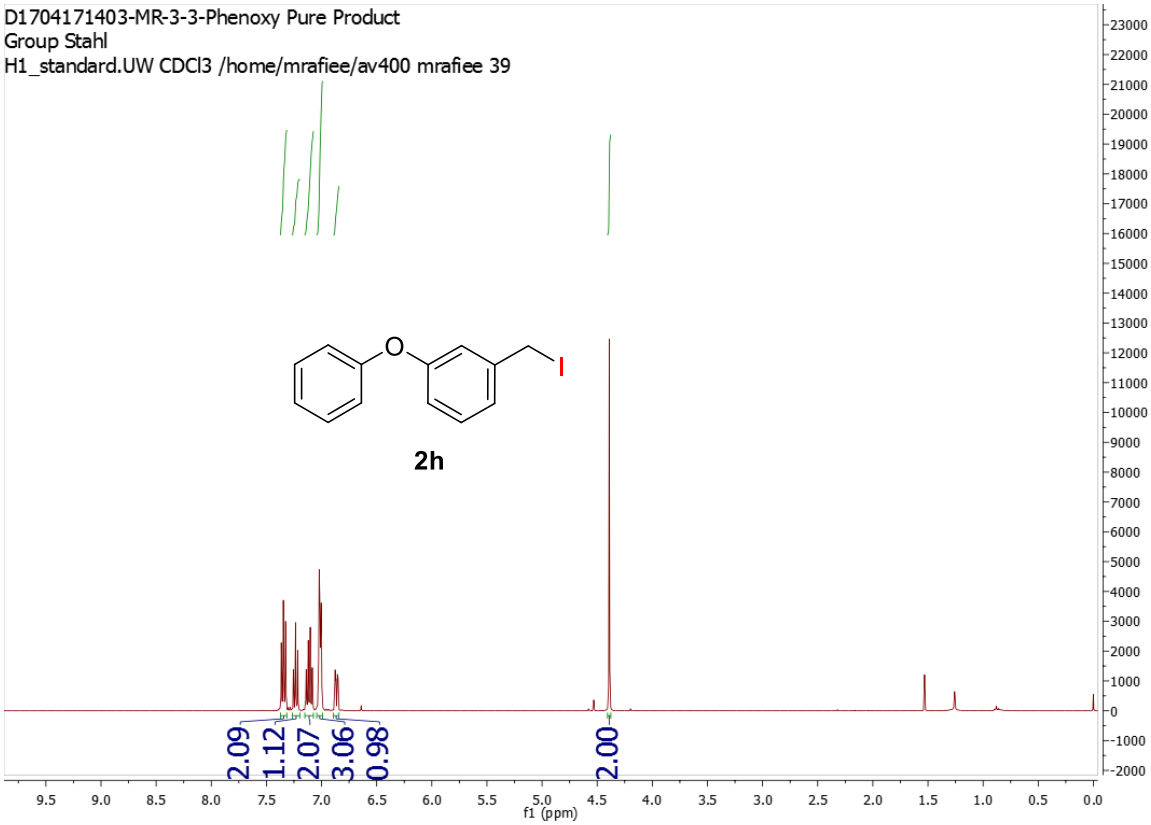
D1704171403-MR-3-3-Phenoxy Pure Product
Group Stahl
H1_standard.UW CDCl3 /home/mrafiee/av400 mrafiee 39
O
I
2h
2.09
1.12
2.07
3.06
0.98
2.00
f1 (ppm)

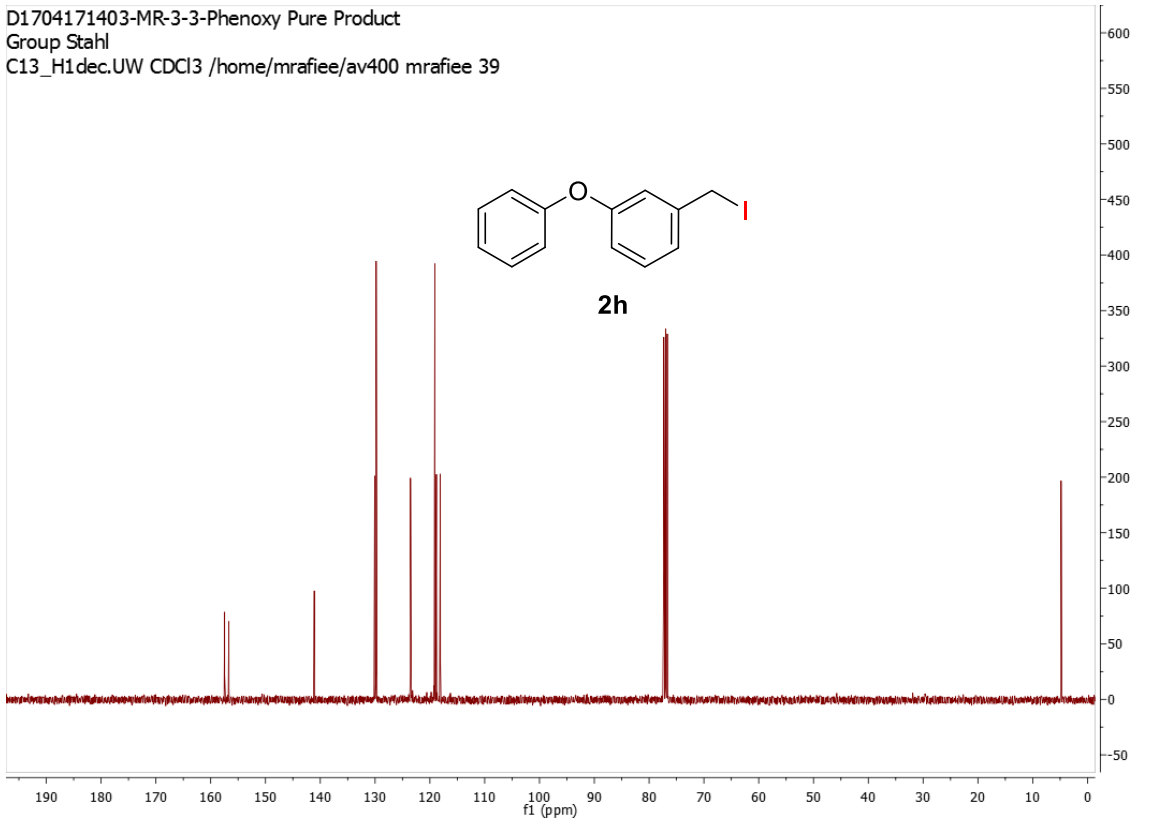
D1704171403-MR-3-3-Phenoxy Pure Product
Group Stahl
C13_H1dec.UW CDCl3 /home/mrafiee/av400 mrafiee 39
O
I
2h
f1 (ppm)

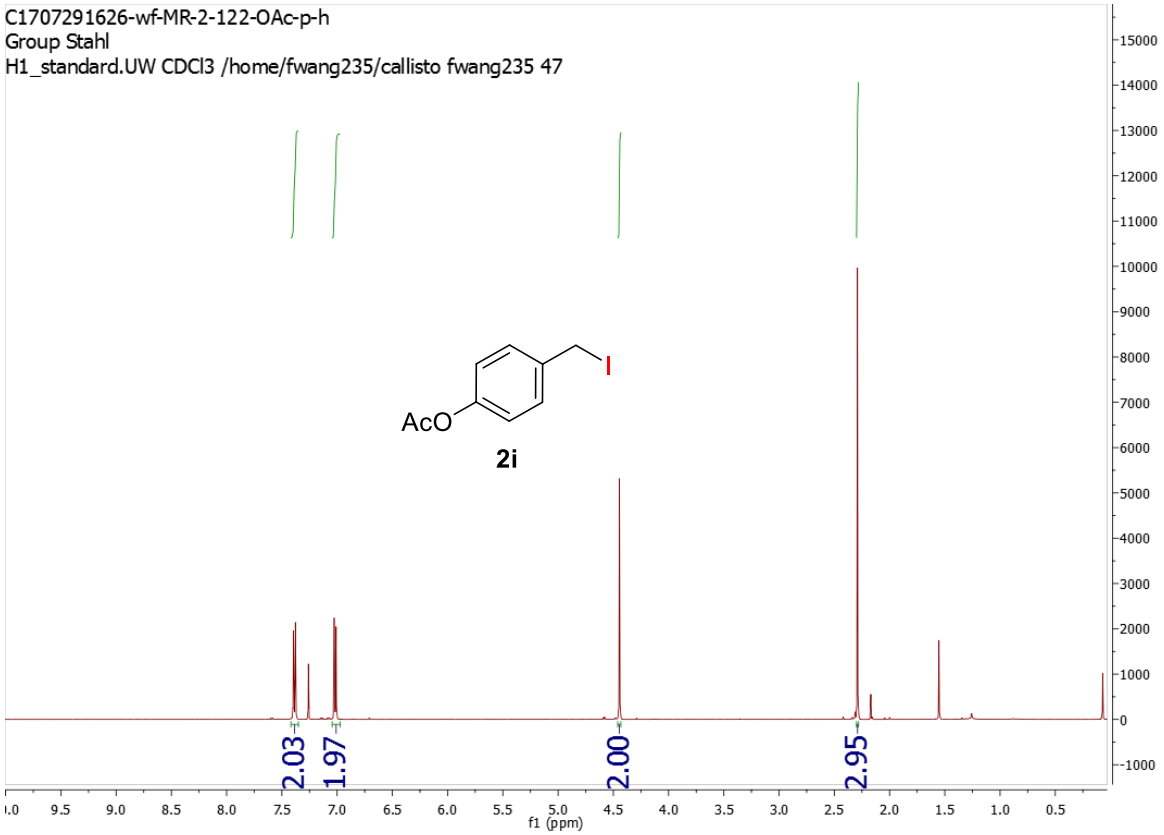
C1707291626-wf-MR-2-122-OAc-p-h
Group Stahl
H1_standard.UW CDCl3 /home/fwang235/callisto fwang235 47
AcO
I
2i
2.03
1.97
2.00
2.95
f1 (ppm)

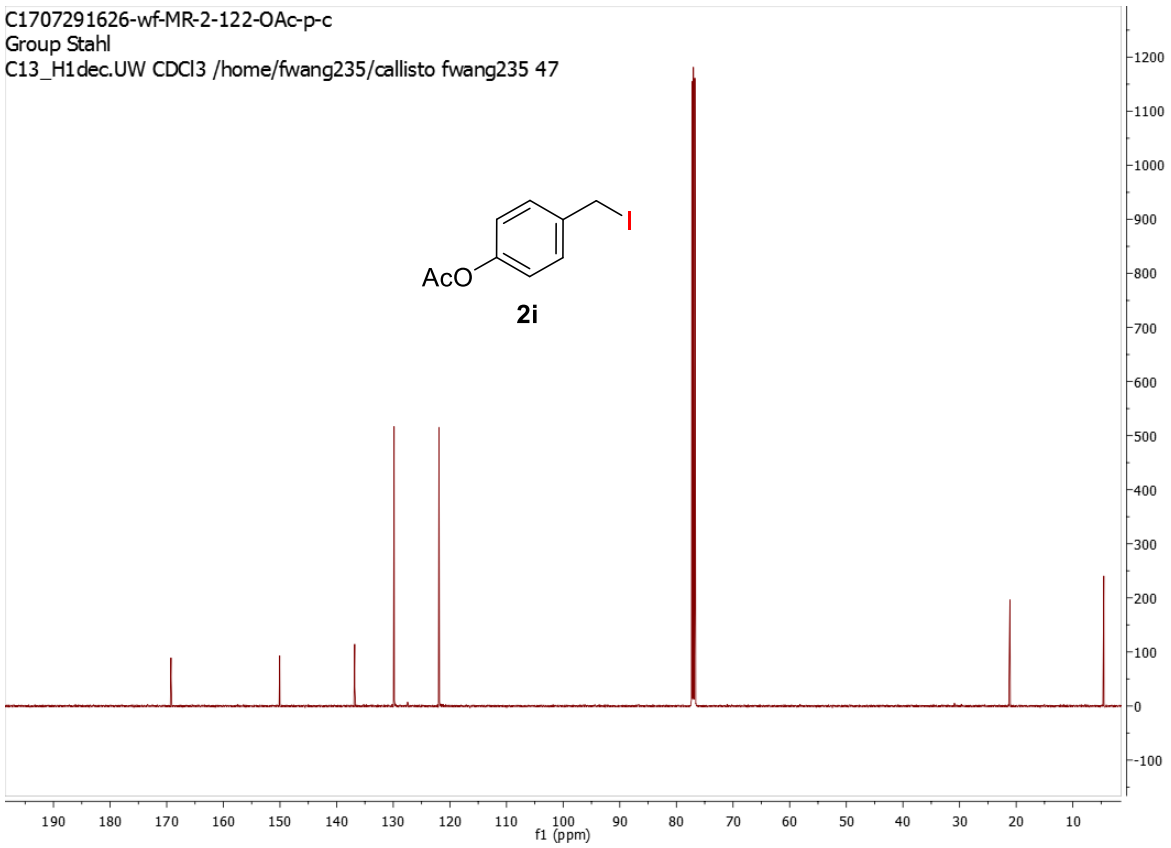
C1707291626-wf-MR-2-122-OAc-p-c
Group Stahl
C13_H1dec.UW CDCl3 /home/fwang235/callisto fwang235 47
AcO
I
2i
f1 (ppm)

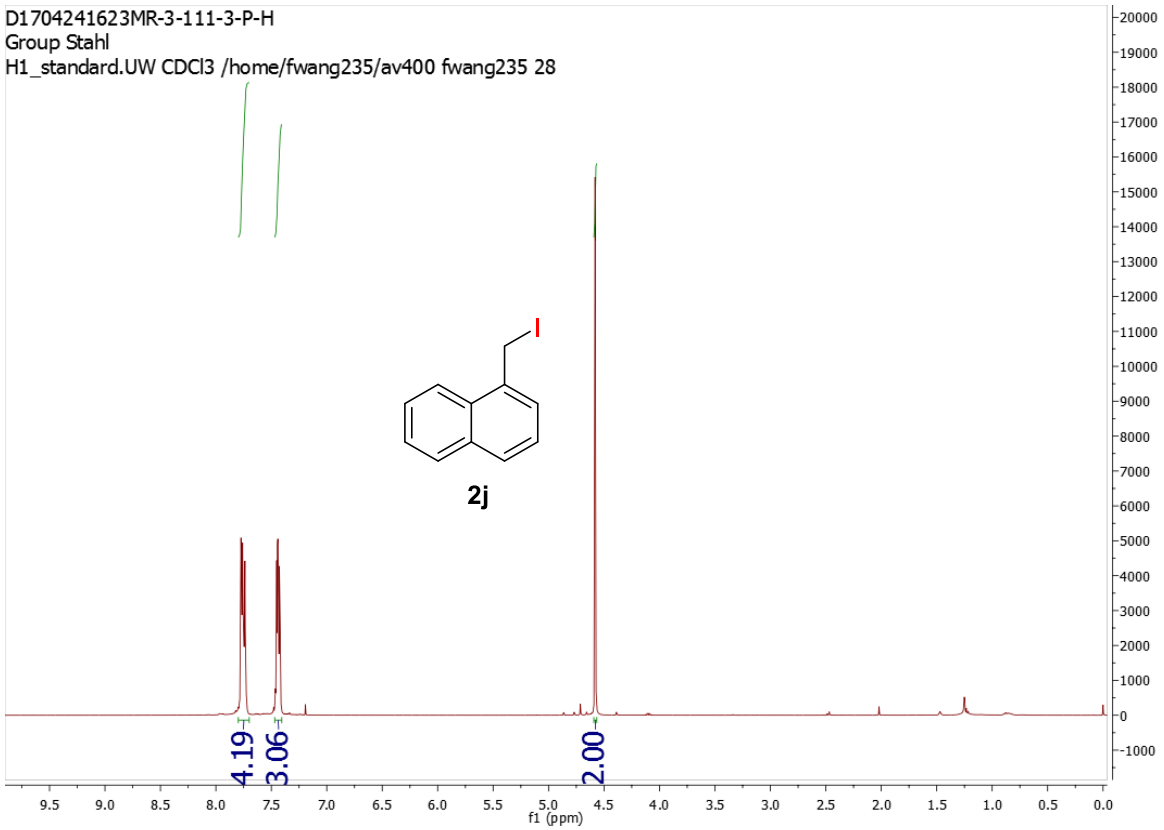
D1704241623MR-3-111-3-P-H
Group Stahl
H1_standard.UW CDCl3 /home/fwang235/av400 fwang235 28
I
2j
4.19
3.06
2.00
f1 (ppm)

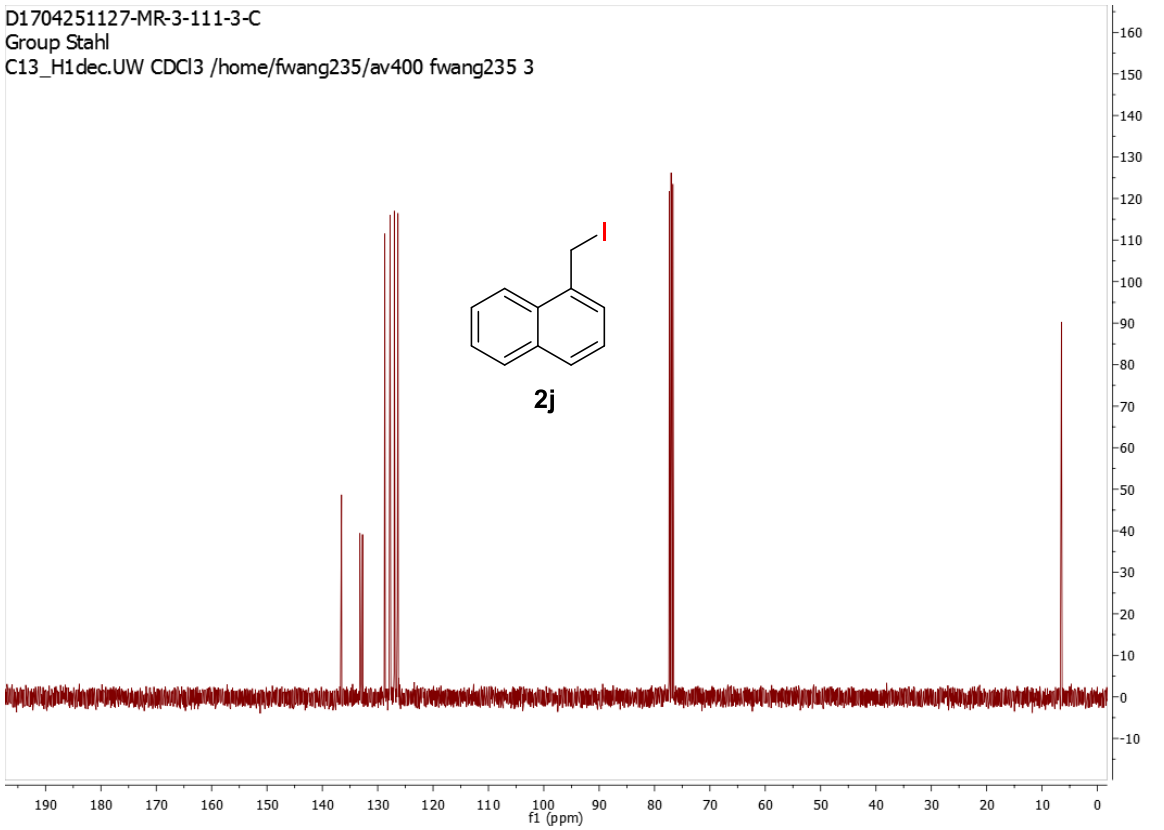
D1704251127-MR-3-111-3-C
Group Stahl
C13_H1dec.UW CDCl3 /home/fwang235/av400 fwang235 3
I
2j
f1 (ppm)

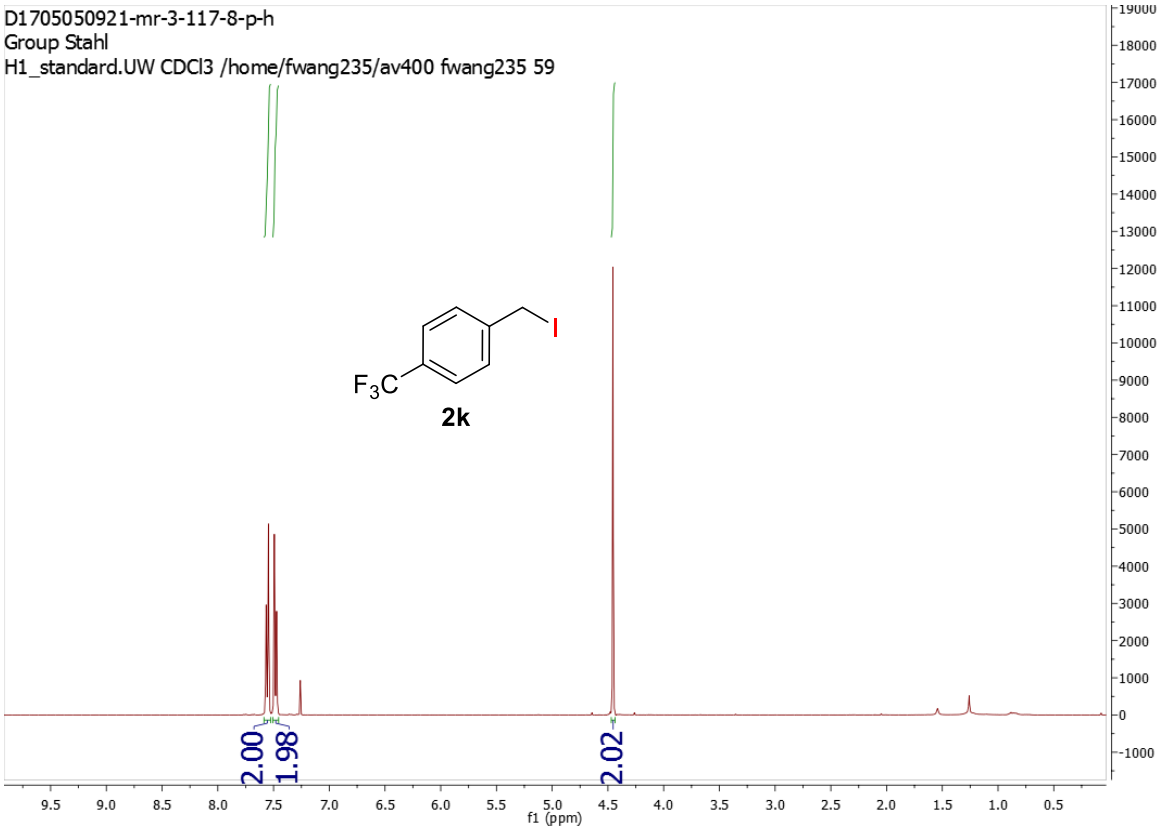
D1705050921-mr-3-117-8-p-h
Group Stahl
H1_standard.UW CDCl3 /home/fwang235/av400 fwang235 59
F3C
I
2k
2.00
1.98
2.02
f1 (ppm)

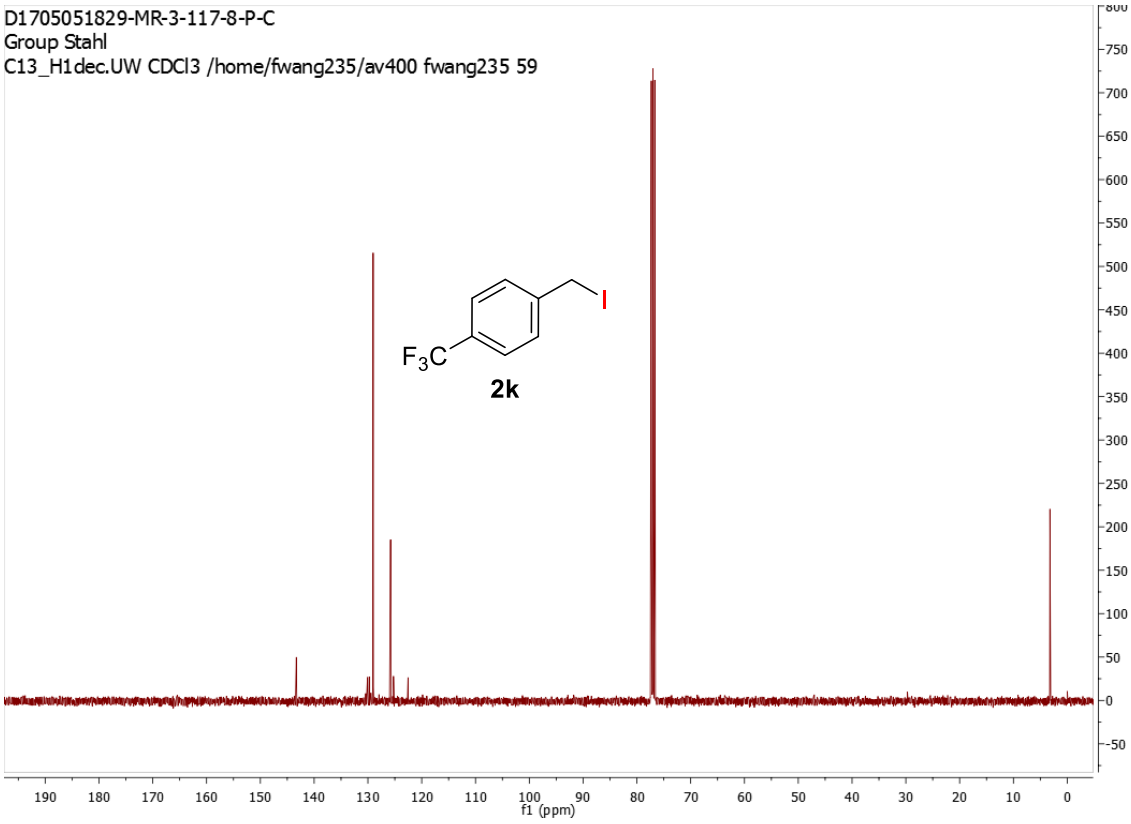
D1705051829-MR-3-117-8-P-C
Group Stahl
C13_H1dec.UW CDCl3 /home/fwang235/av400 fwang235 59
F3C
I
2k
f1 (ppm)

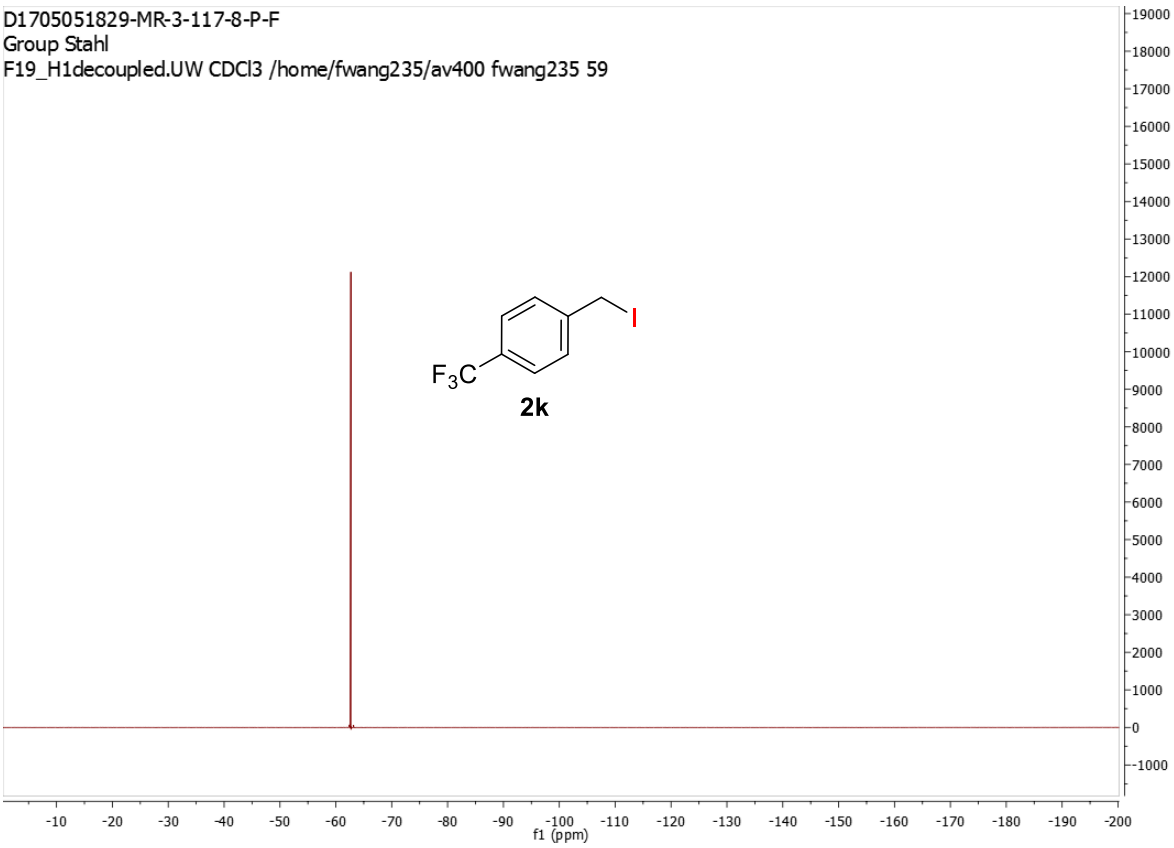
D1705051829-MR-3-117-8-P-F
Group Stahl
F19_H1decoupled.UW CDCl3 /home/fwang235/av400 fwang235 59
F3C
I
2k
f1 (ppm)

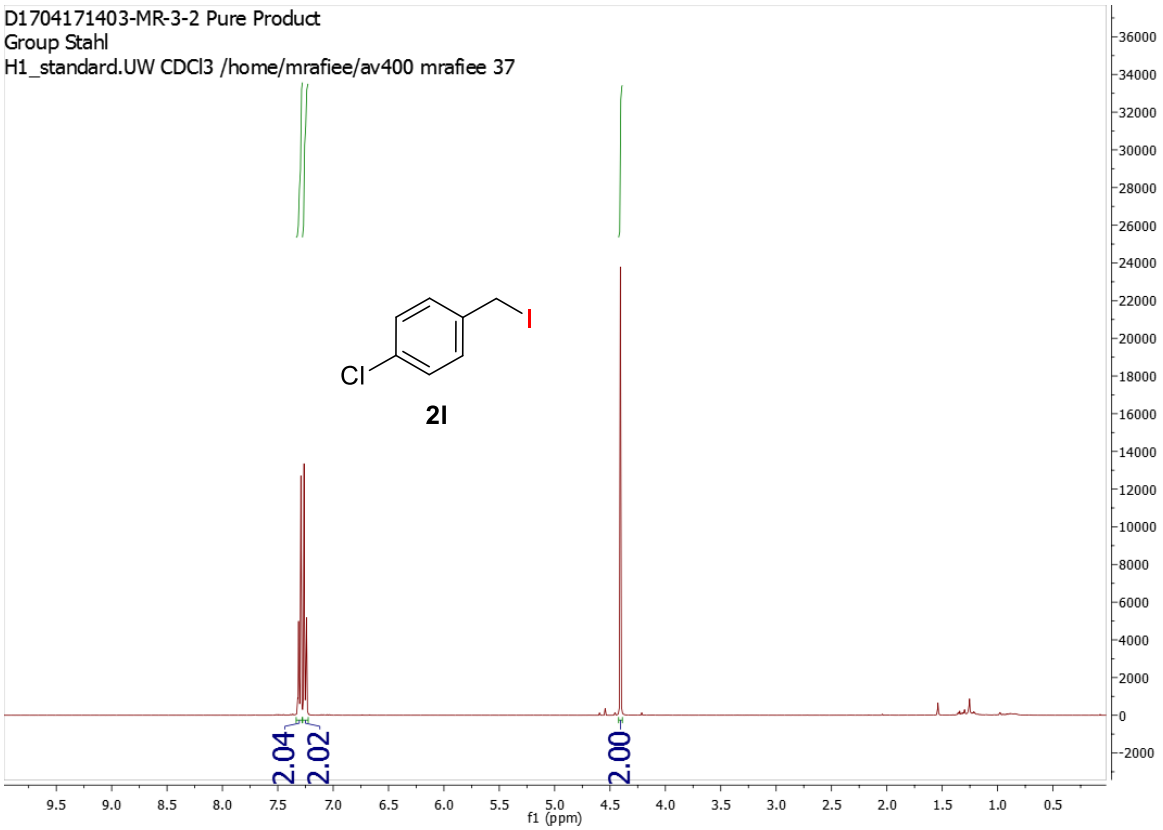
D1704171403-MR-3-2 Pure Product
Group Stahl
H1_standard.UW CDCl3 /home/mrafiee/av400 mrafiee 37
Cl
I
2l
2.04
2.02
2.00
f1 (ppm)

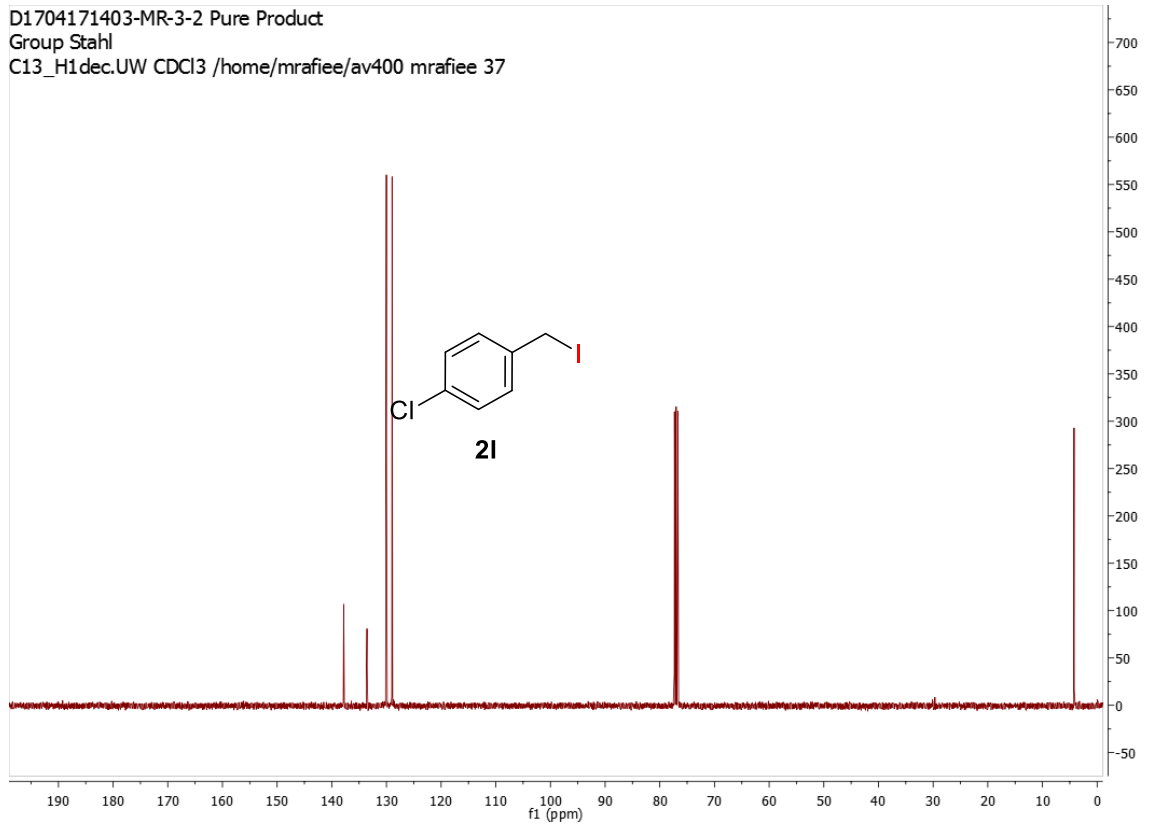
D1704171403-MR-3-2 Pure Product
Group Stahl
C13_H1dec.UW CDCl3 /home/mrafiee/av400 mrafiee 37
Cl
I
2l
f1 (ppm)

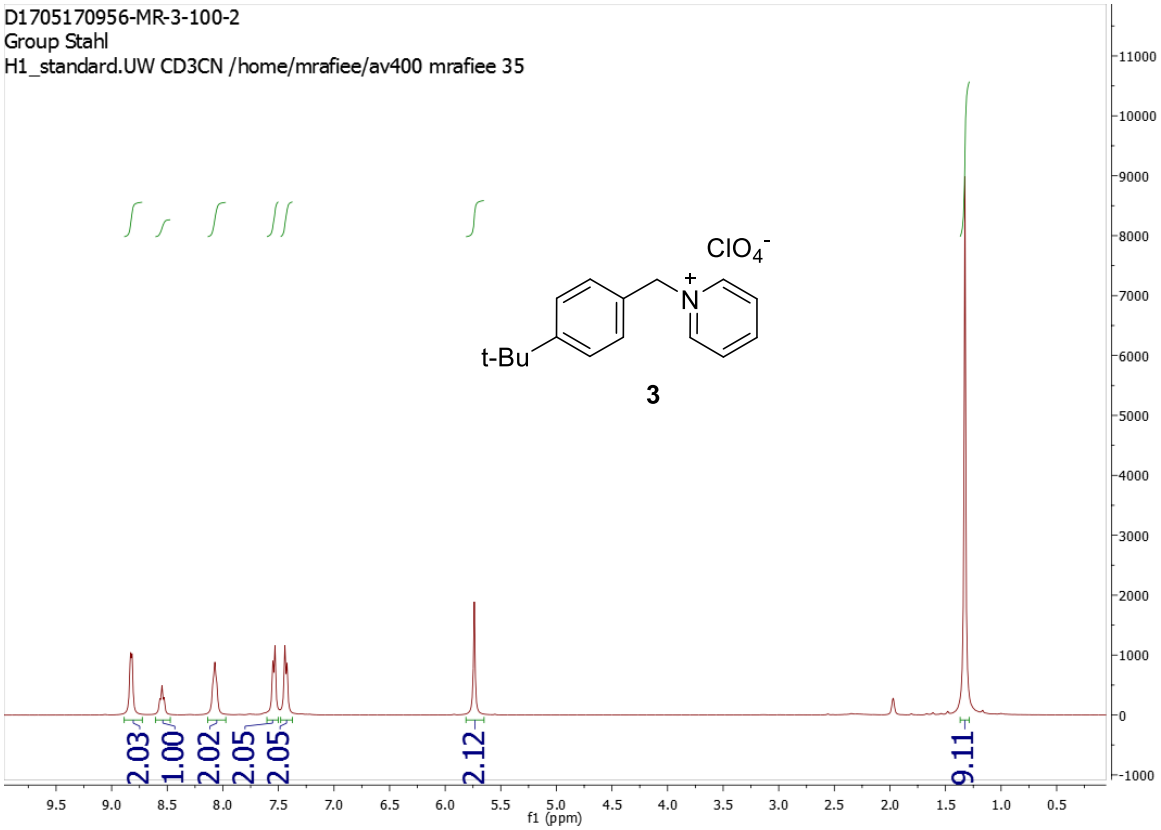
D1705170956-MR-3-100-2
Group Stahl
H1_standard.UW CD3CN /home/mrafiee/av400 mrafiee 35
ClO4-
N+
t-Bu
3
2.03
1.00
2.02
2.05
2.05
2.12
9.11
f1 (ppm)

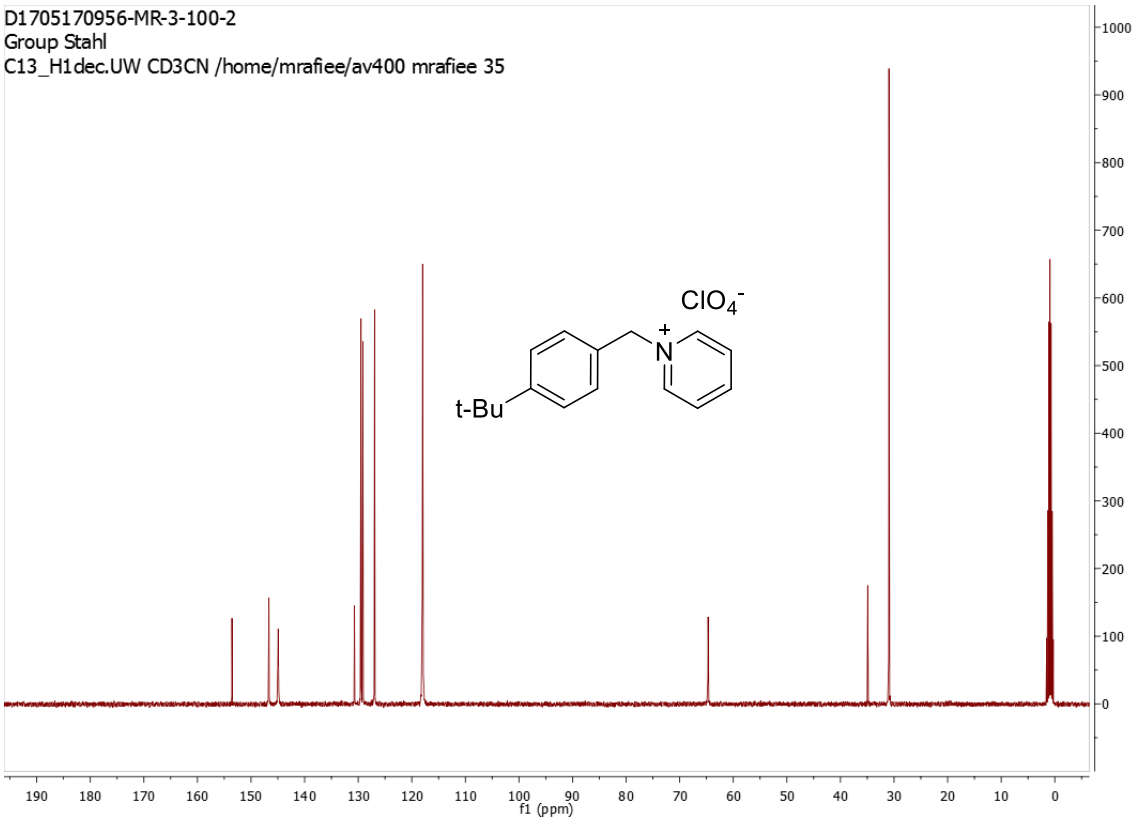
D1705170956-MR-3-100-2
Group Stahl
C13_H1dec.UW CD3CN /home/mrafiee/av400 mrafiee 35
ClO4-
N+
t-Bu
f1 (ppm)

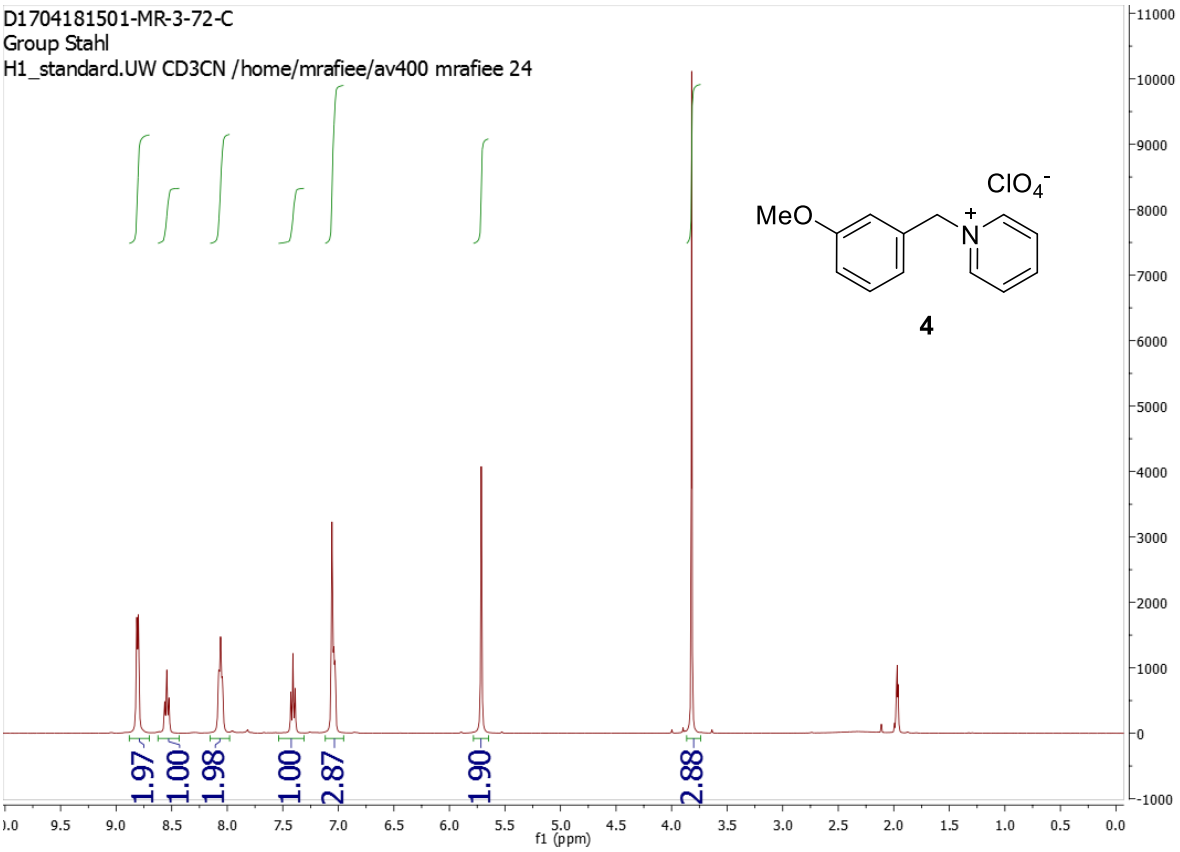
D1704181501-MR-3-72-C
Group Stahl
H1_standard.UW CD3CN /home/mrafiee/av400 mrafiee 24
MeO
ClO4-
N+
4
1.97
1.00
1.98
1.00
2.87
1.90
2.88
f1 (ppm)

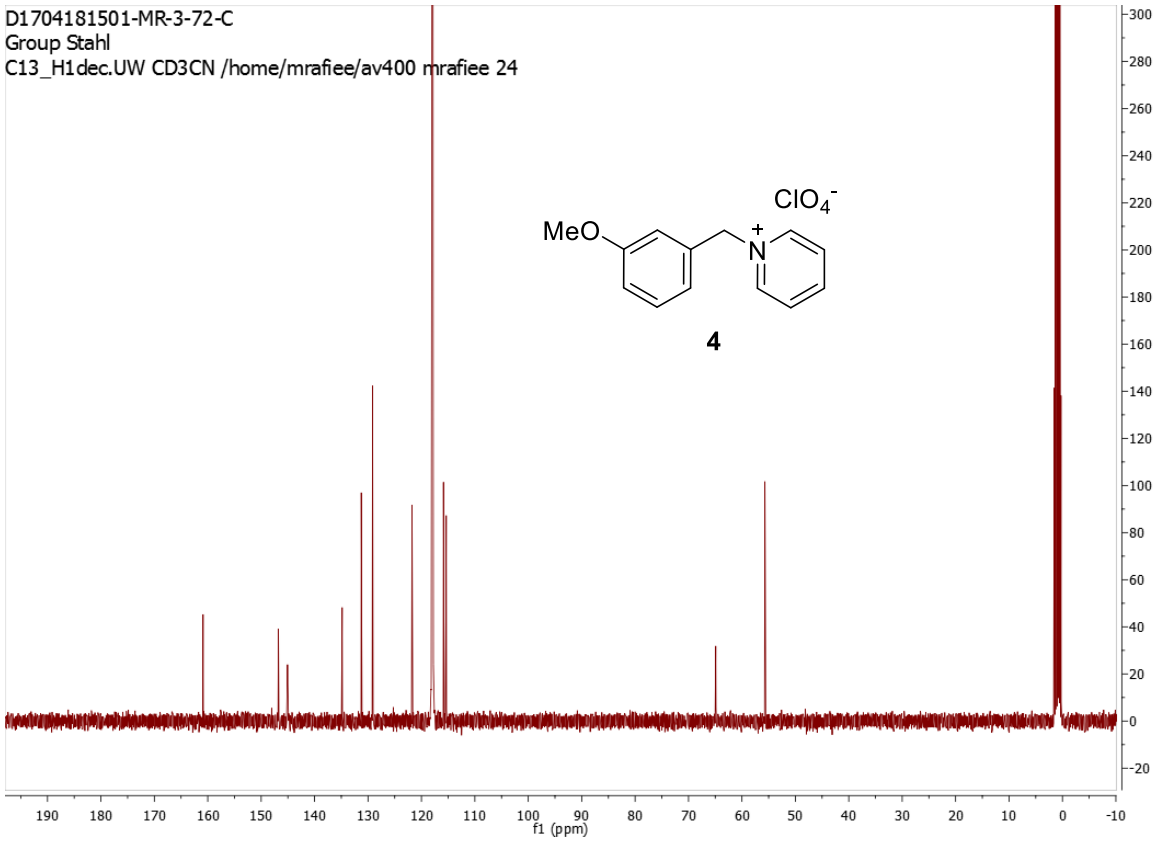
D1704181501-MR-3-72-C
Group Stahl
C13_H1dec.UW CD3CN /home/mrafiee/av400 mrafiee 24
MeO
ClO4-
N+
4
f1 (ppm)

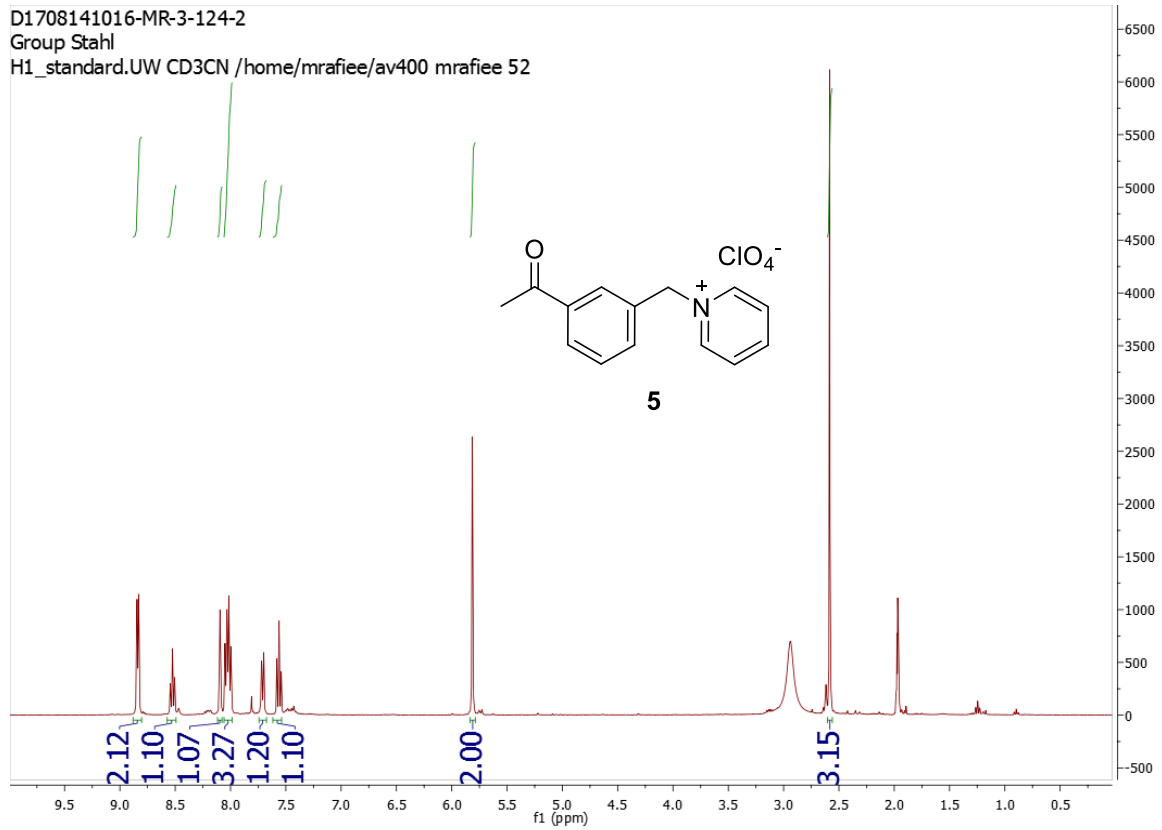
D1708141016-MR-3-124-2
Group Stahl
H1_standard.UW CD3CN /home/mrafiee/av400 mrafiee 52
O
ClO4-
N+
5
2.12
1.10
1.07
3.27
1.20
1.10
2.00
3.15
f1 (ppm)

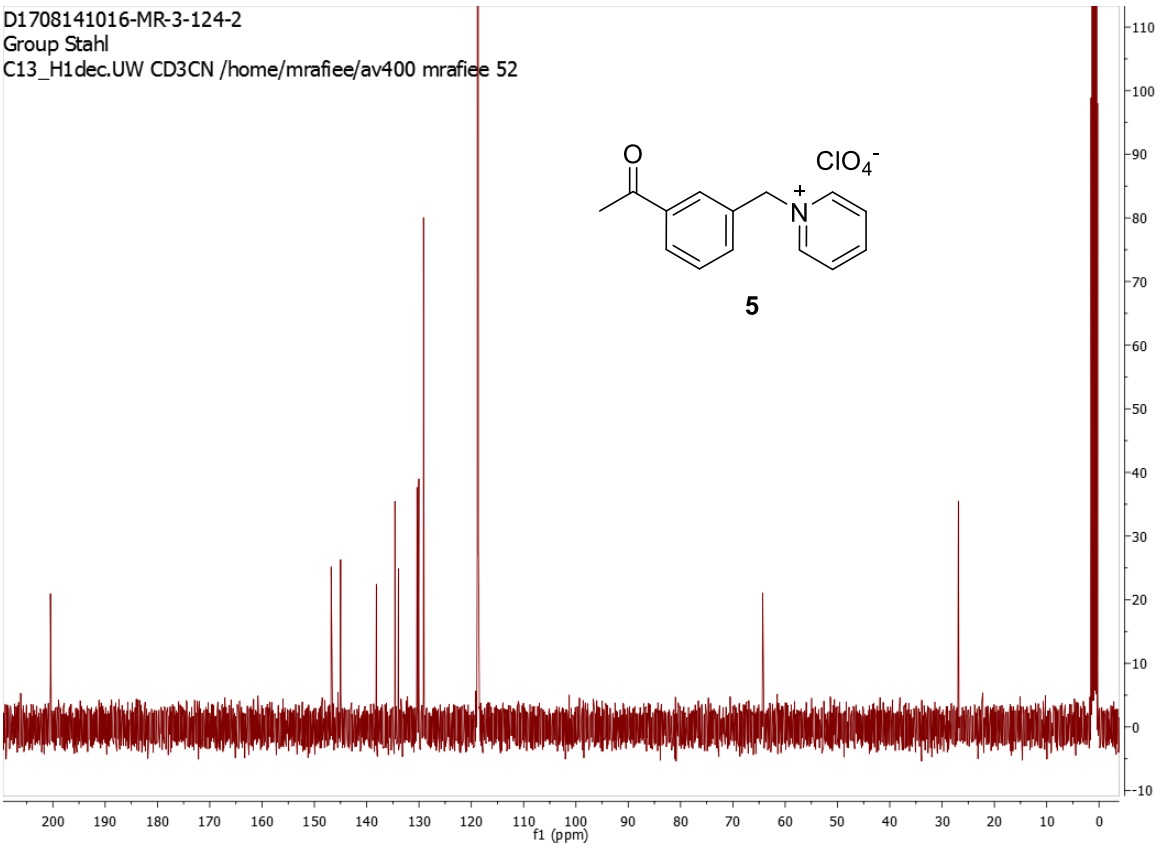
D1708141016-MR-3-124-2
Group Stahl
C13_H1dec.UW CD3CN /home/mrafiee/av400 mrafiee 52
O
ClO4-
N+
5
f1 (ppm)

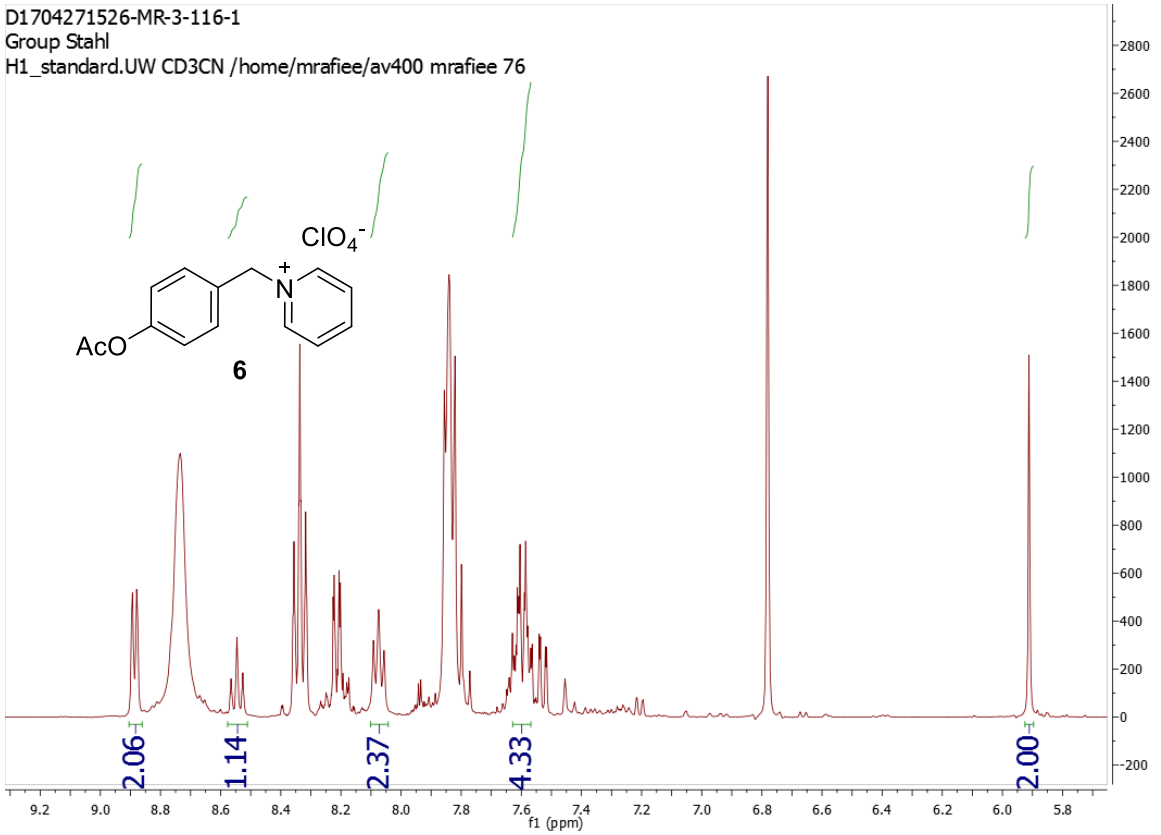
D1704271526-MR-3-116-1
Group Stahl
H1_standard.UW CD3CN /home/mrafiee/av400 mrafiee 76
ClO4-
N+
AcO
6
2.06
1.14
2.37
4.33
2.00
f1 (ppm)

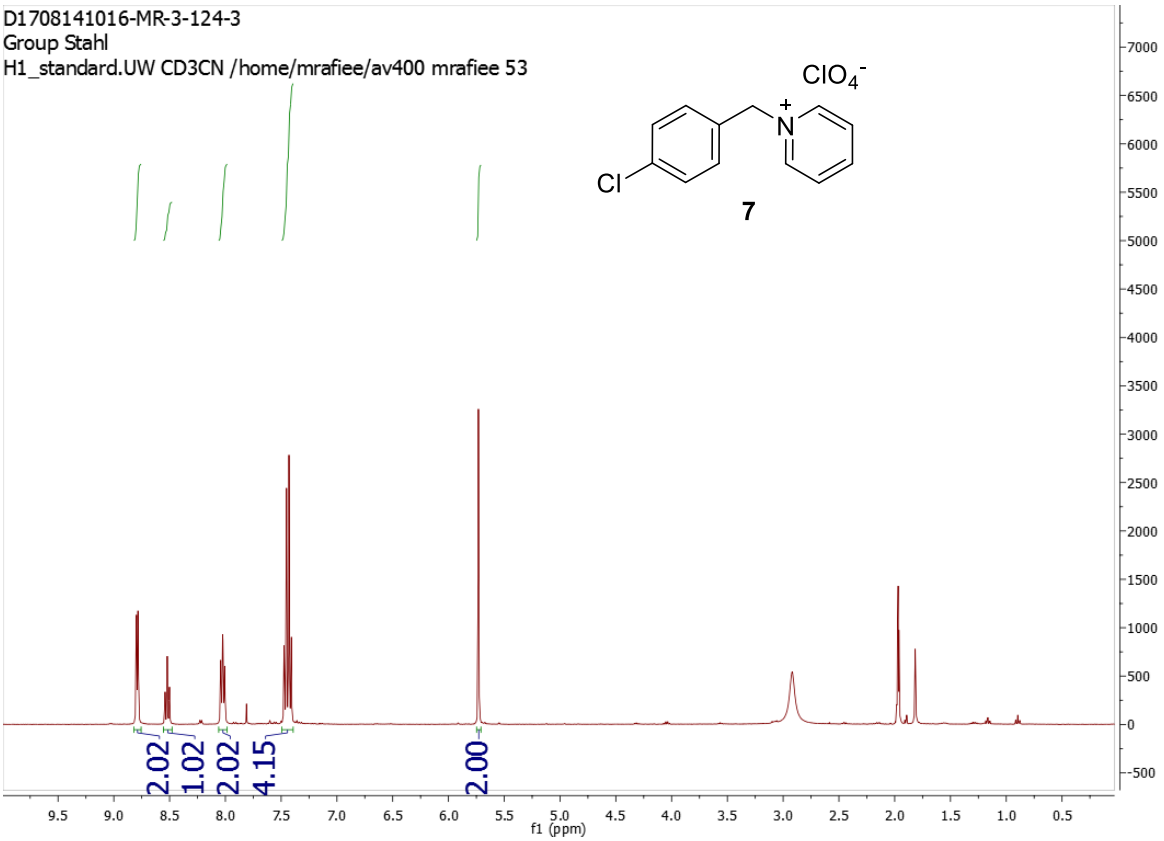
D1708141016-MR-3-124-3
Group Stahl
H1_standard.UW CD3CN /home/mrafiee/av400 mrafiee 53
ClO4-
N+
Cl
7
2.02
1.02
2.02
4.15
2.00
f1 (ppm)

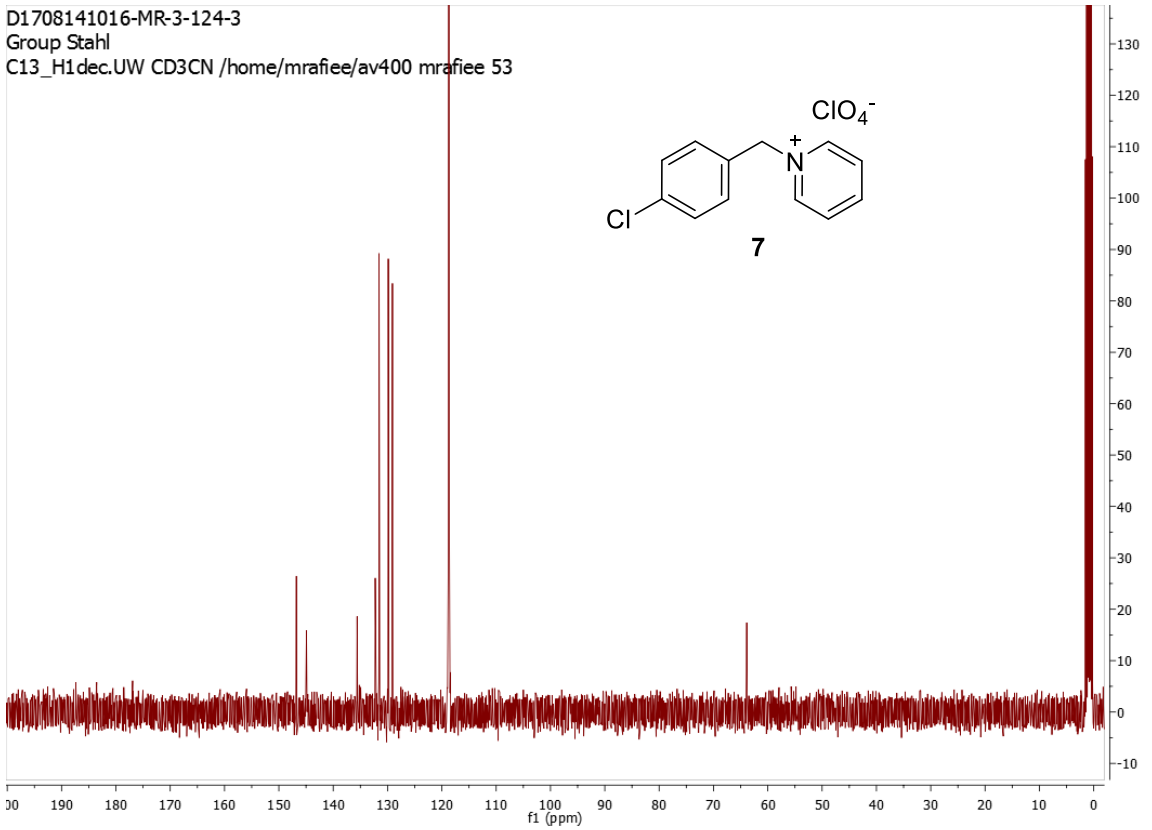
D1708141016-MR-3-124-3
Group Stahl
C13_H1dec.UW CD3CN /home/mrafiee/av400 mrafiee 53
ClO4-
N+
Cl
7
f1 (ppm)

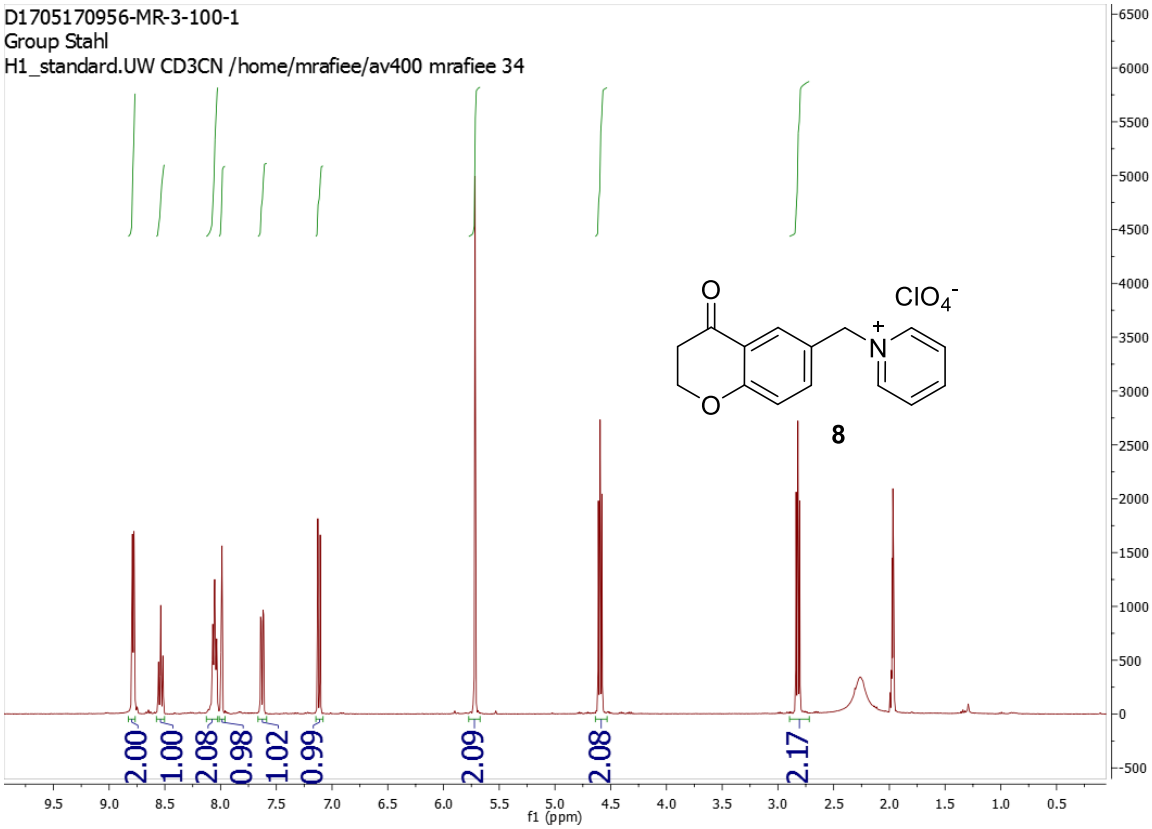
D1705170956-MR-3-100-1
Group Stahl
H1_standard.UW CD3CN /home/mrafiee/av400 mrafiee 34
O
O
ClO4-
N+
8
2.00
1.00
2.08
0.98
1.02
0.99
2.09
2.08
2.17
f1 (ppm)

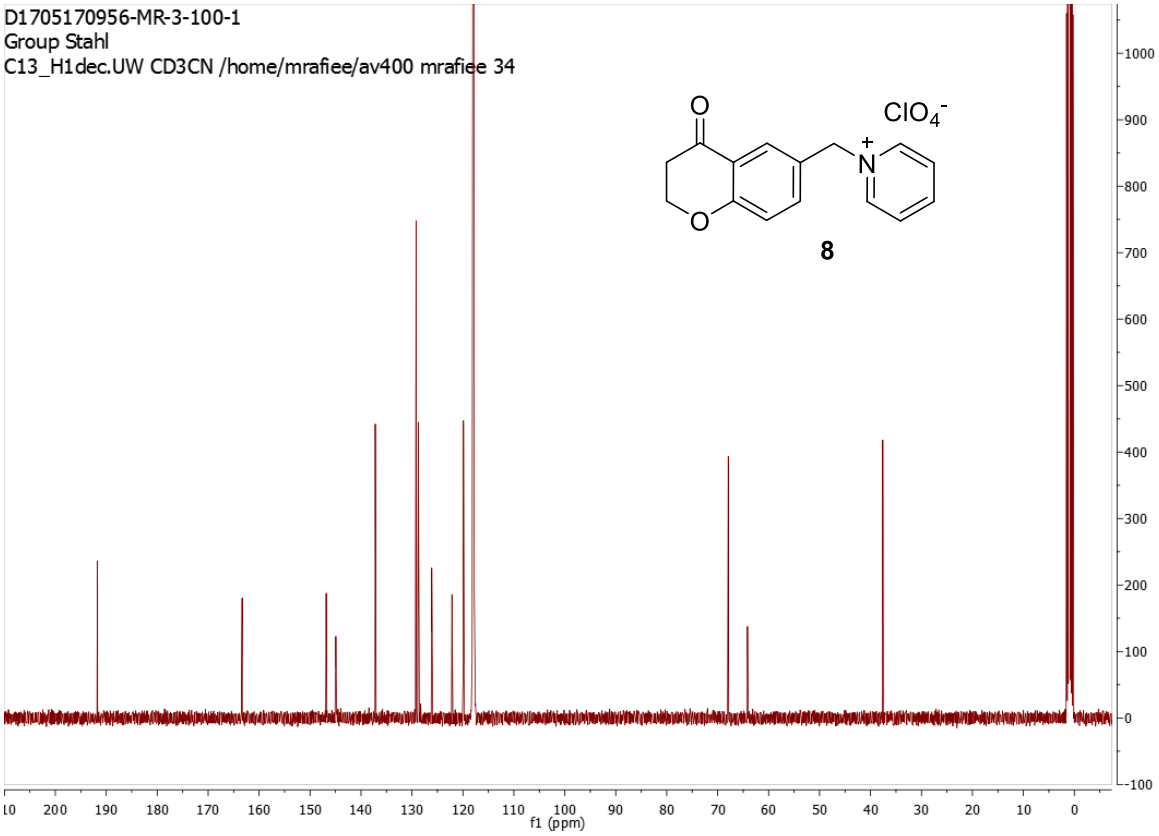
D1705170956-MR-3-100-1
Group Stahl
C13_H1dec.UW CD3CN /home/mrafiee/av400 mrafiee 34
O
O
N+
ClO4-
8
1000
900
800
700
600
500
400
300
200
100
0
-100
10 200 190 180 170 160 150 140 130 120 110 100 90 80 70 60 50 40 30 20 10 0
f1 (ppm)

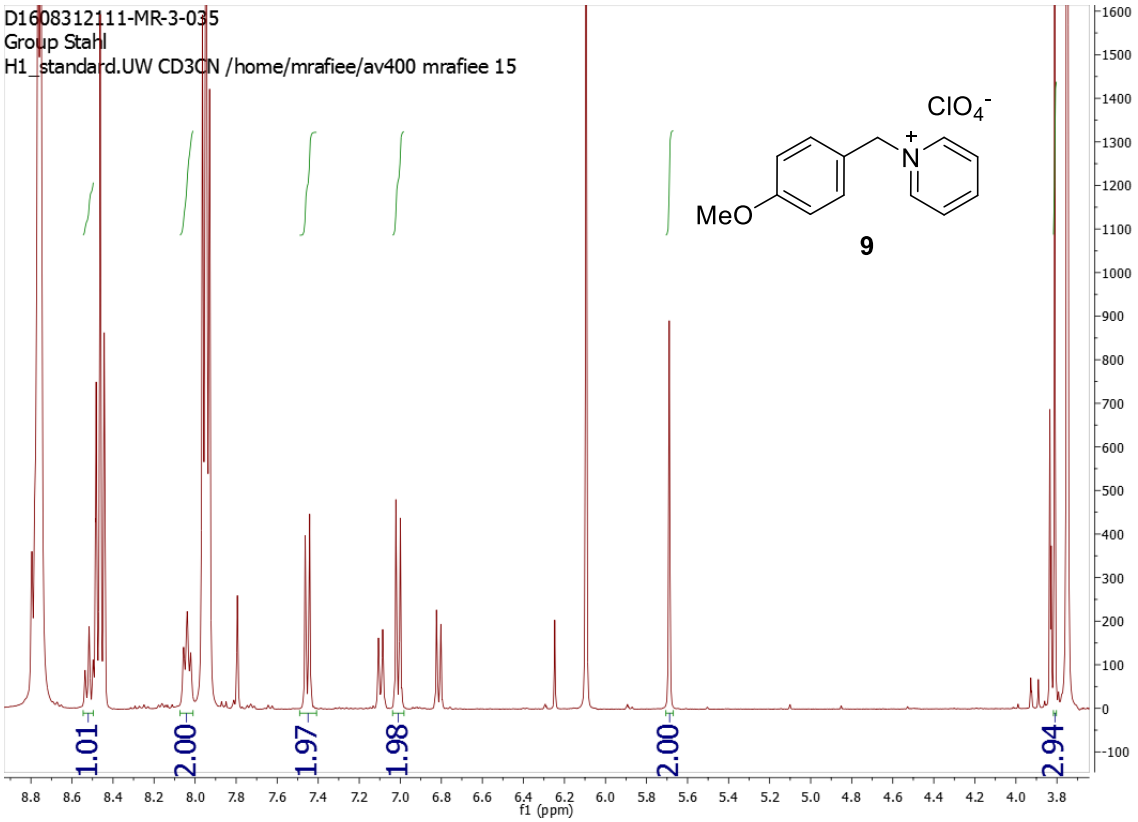
D1608312111-MR-3-035
Group Stahl
H1_standard.UW CD3CN /home/mrafiee/av400 mrafiee 15
ClO4-
N+
MeO
9
1.01
2.00
1.97
1.98
2.00
2.94
f1 (ppm)

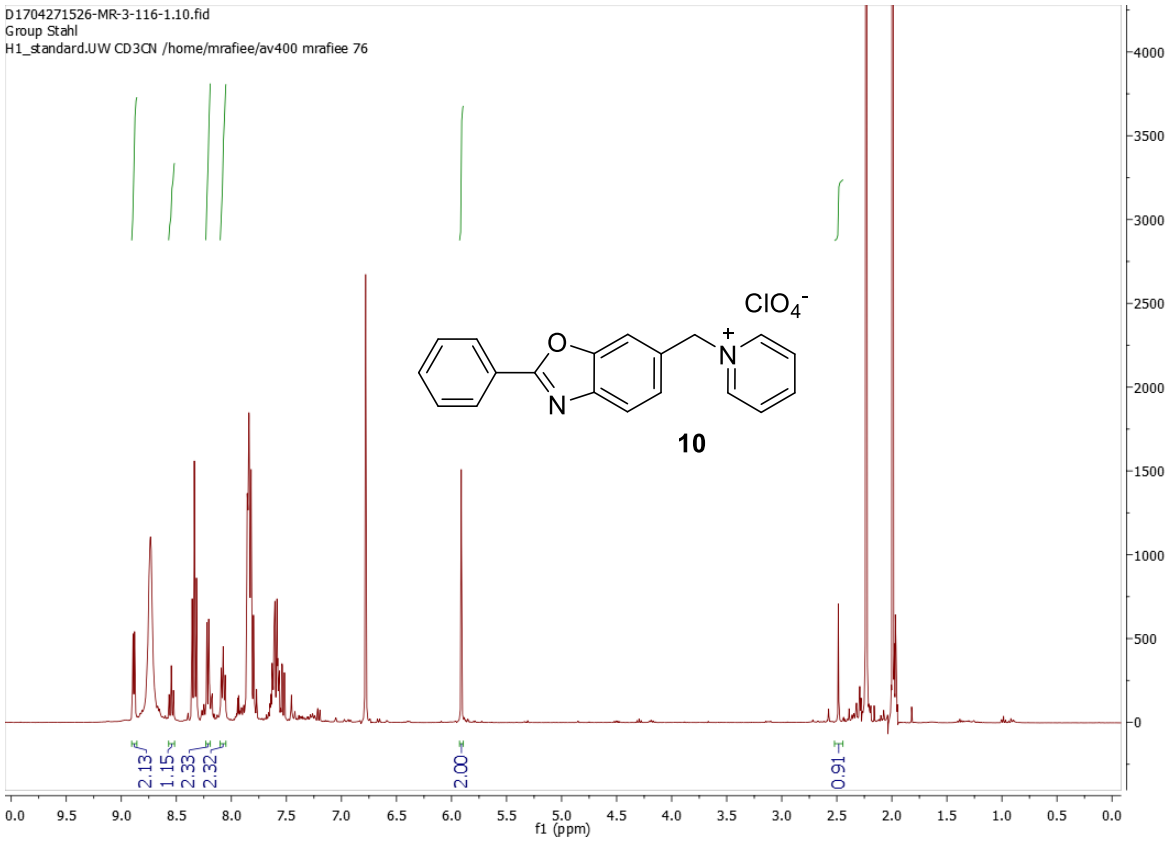
D1704271526-MR-3-116-1.10.fid
Group Stahl
H1_standard.UW CD3CN /home/mrafiee/av400 mrafiee 76
ClO4-
O
N
N+
10
2.13
1.15
2.33
2.32
2.00
0.91
f1 (ppm)

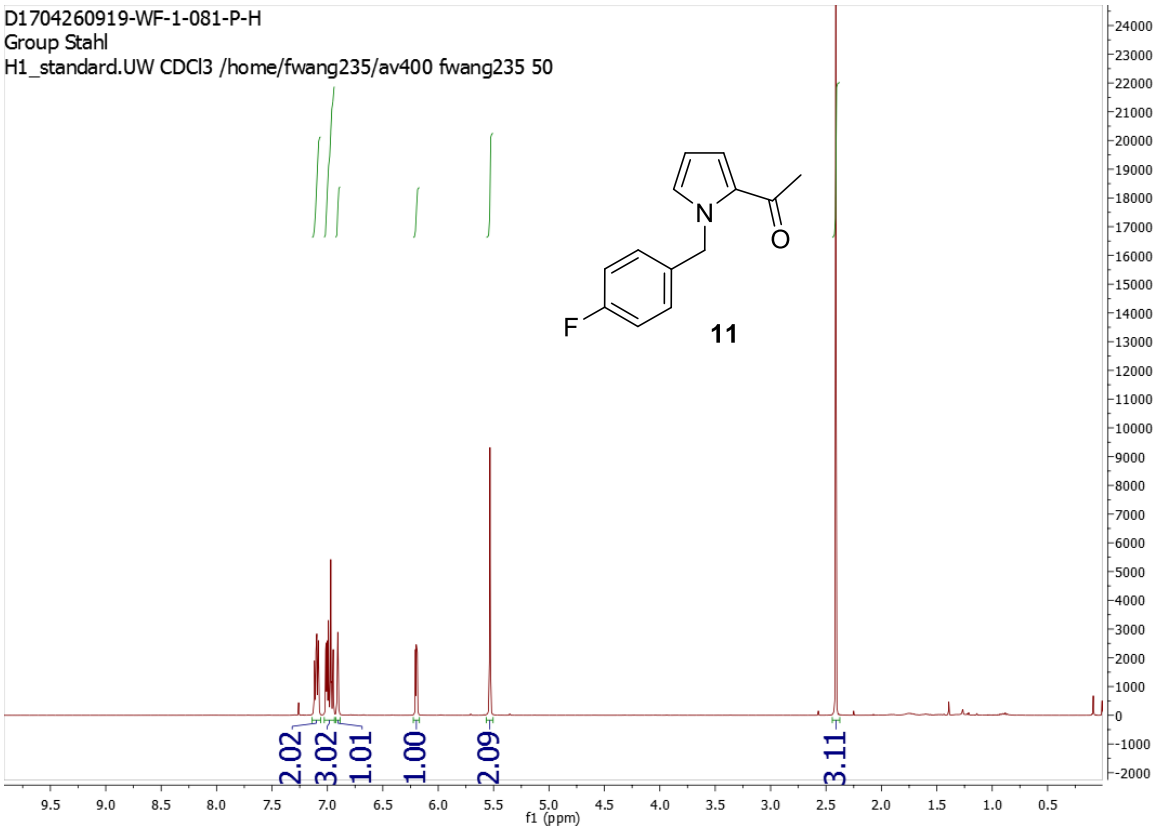
D1704260919-WF-1-081-P-H
Group Stahl
H1_standard.UW CDCl3 /home/fwang235/av400 fwang235 50
N
O
F
11
2.02
3.02
1.01
1.00
2.09
3.11
f1 (ppm)

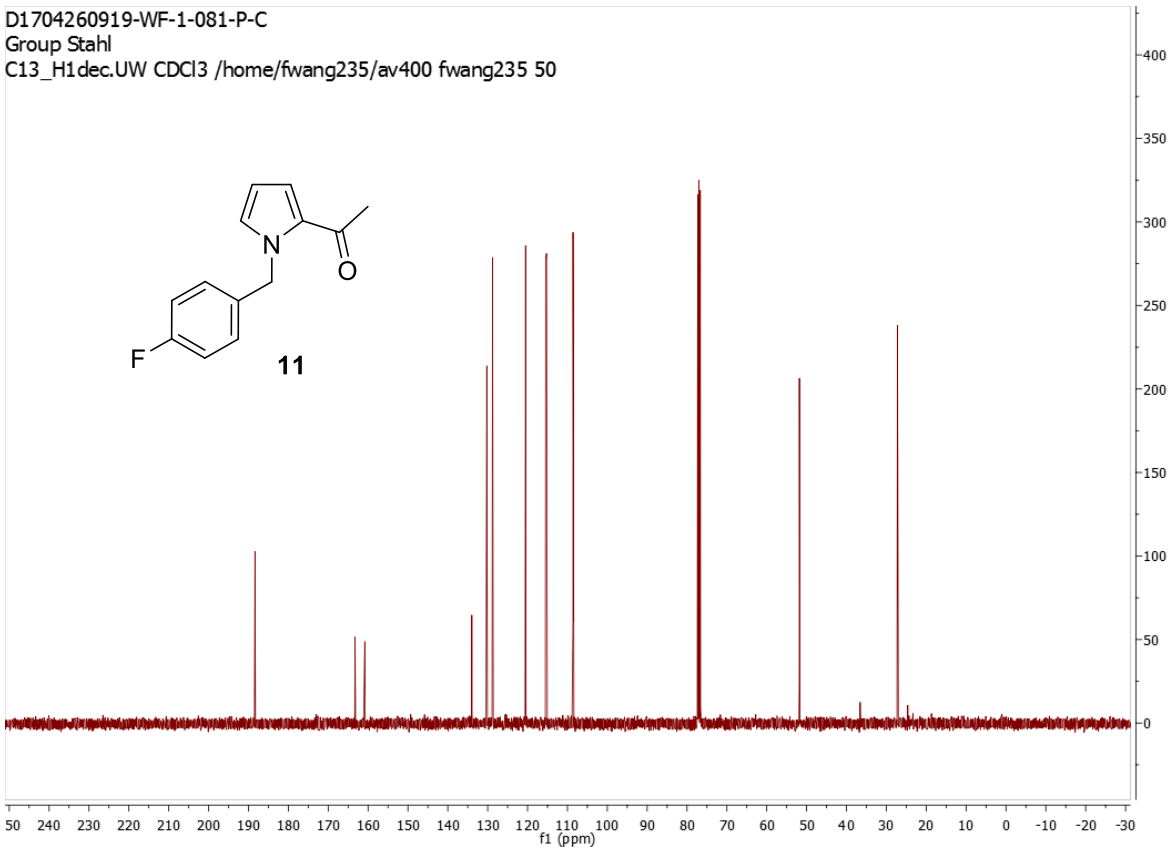
D1704260919-WF-1-081-P-C
Group Stahl
C13_H1dec.UW CDCl3 /home/fwang235/av400 fwang235 50
N
O
F
11
f1 (ppm)

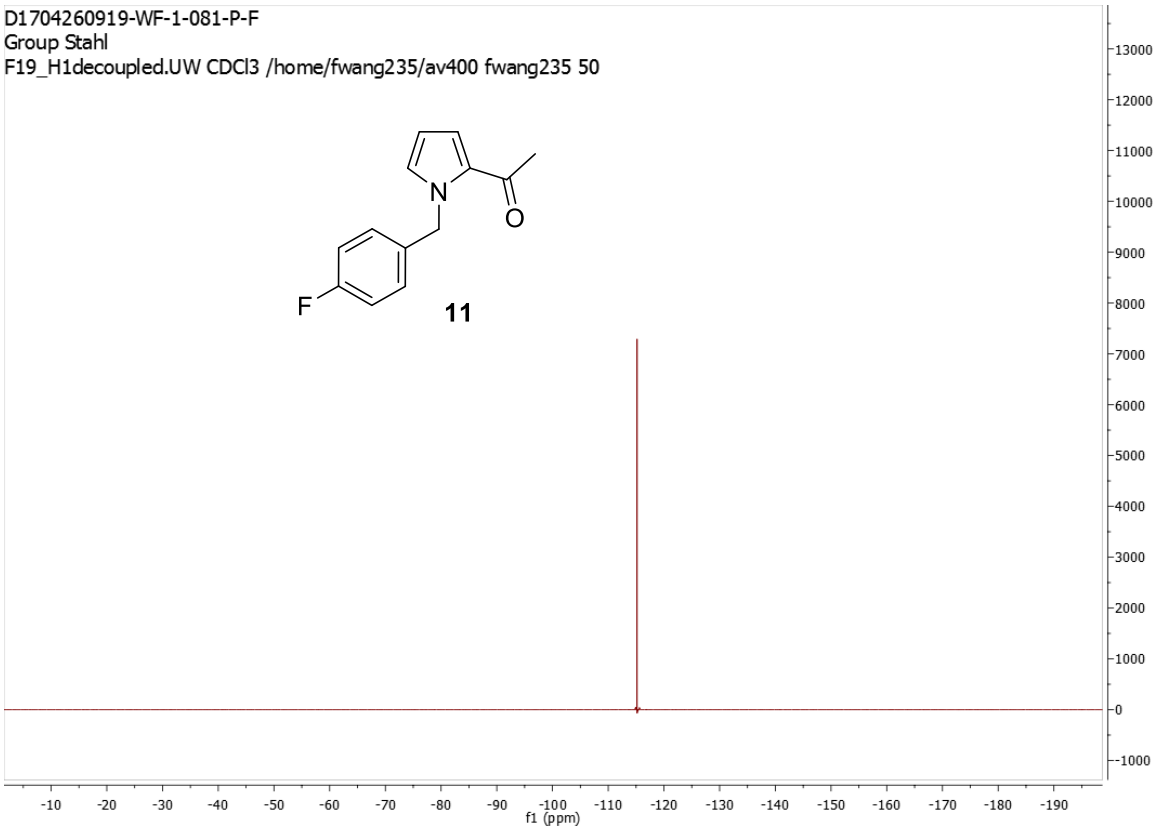
D1704260919-WF-1-081-P-F
Group Stahl
F19_H1decoupled.UW CDCl3 /home/fwang235/av400 fwang235 50
N
O
F
11
f1 (ppm)

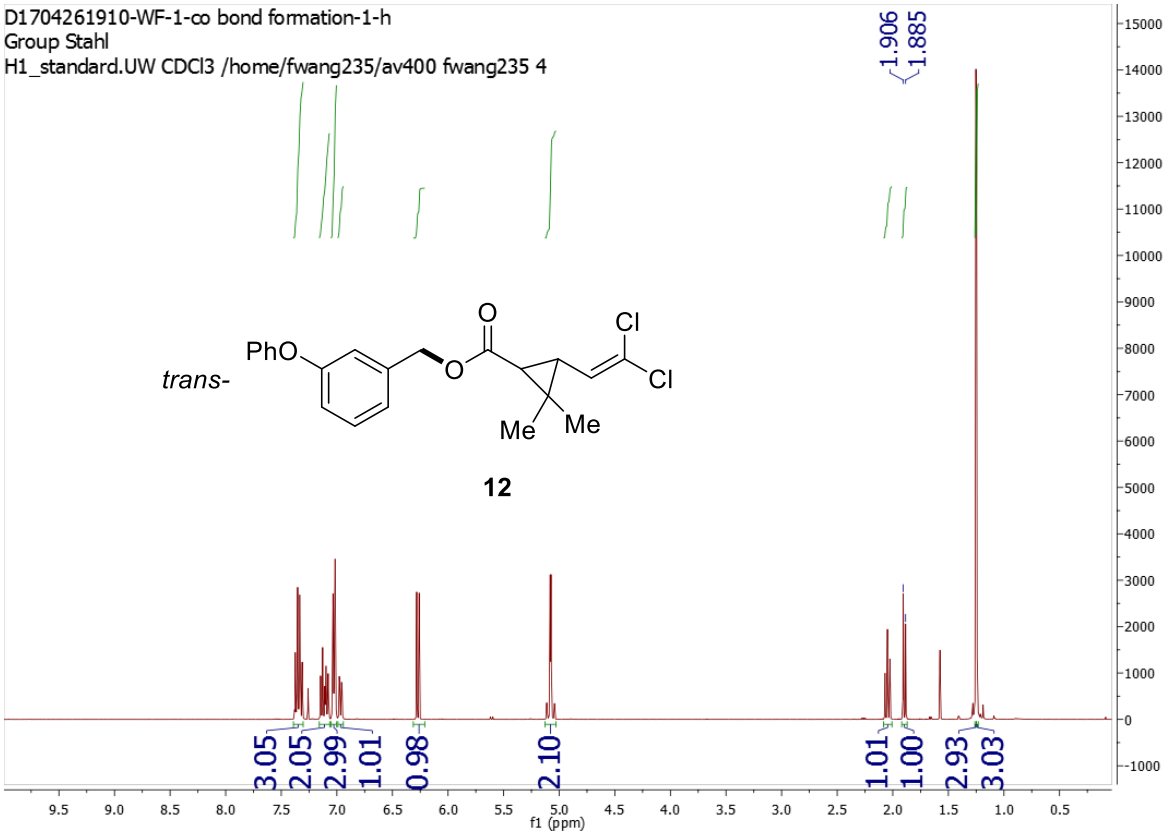
D1704261910-WF-1-co bond formation-1-h
Group Stahl
H1_standard.UW CDCl3 /home/fwang235/av400 fwang235 4
1.906
1.885
trans-
PhO
O
O
Cl
Cl
Me
Me
12
3.05
2.05
2.99
1.01
0.98
2.10
1.01
1.00
2.93
3.03
f1 (ppm)

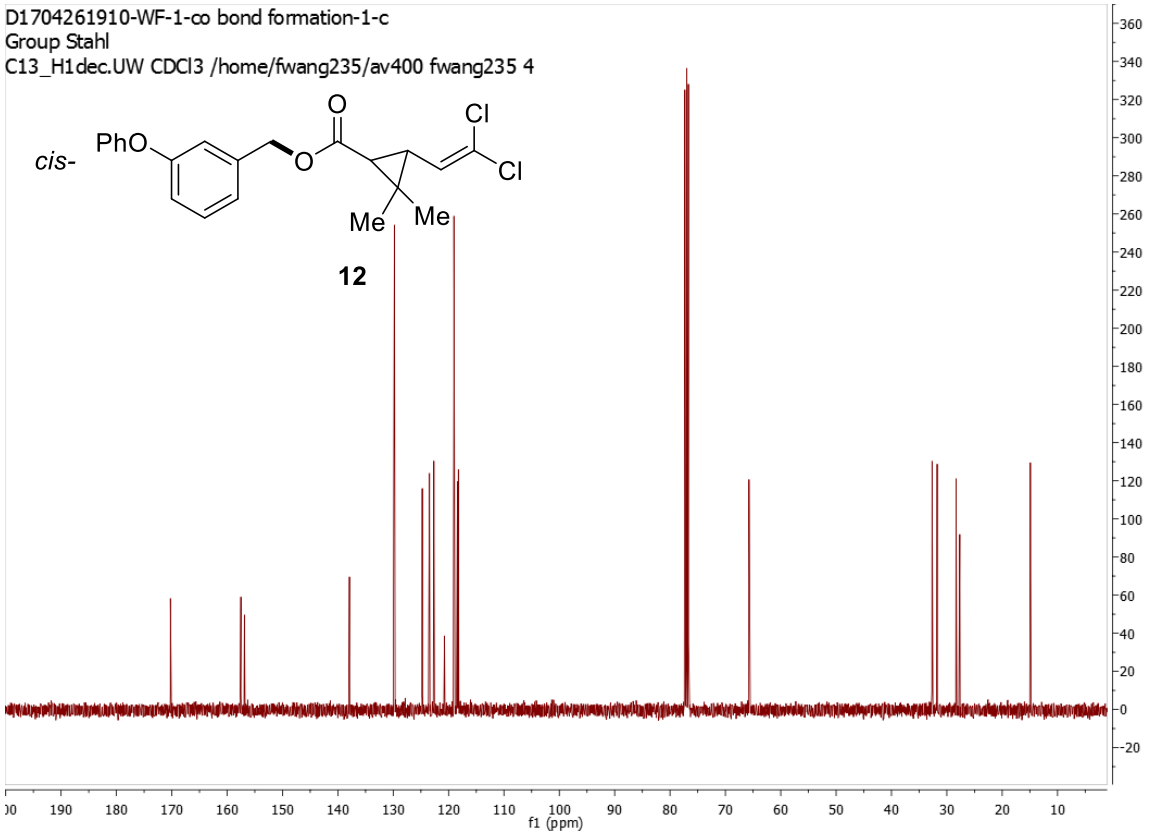
D1704261910-WF-1-co bond formation-1-c
Group Stahl
C13_H1dec.UW CDCl3 /home/fwang235/av400 fwang235 4
cis-
PhO
O
O
Cl
Cl
Me
Me
12
f1 (ppm)

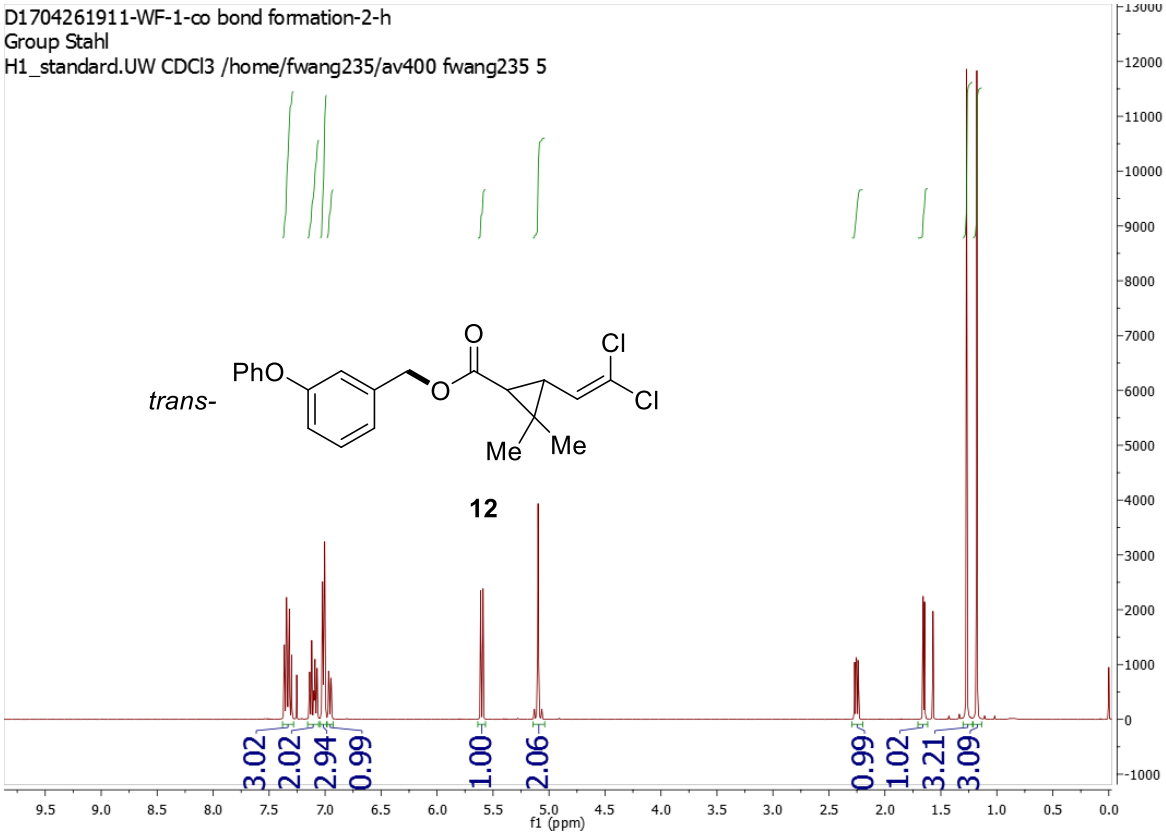
D1704261911-WF-1-co bond formation-2-h
Group Stahl
H1_standard.UW CDCl3 /home/fwang235/av400 fwang235 5
trans-
PhO
O
O
Cl
Cl
Me
Me
12
3.02
2.02
2.94
0.99
1.00
2.06
0.99
1.02
3.21
3.09
f1 (ppm)

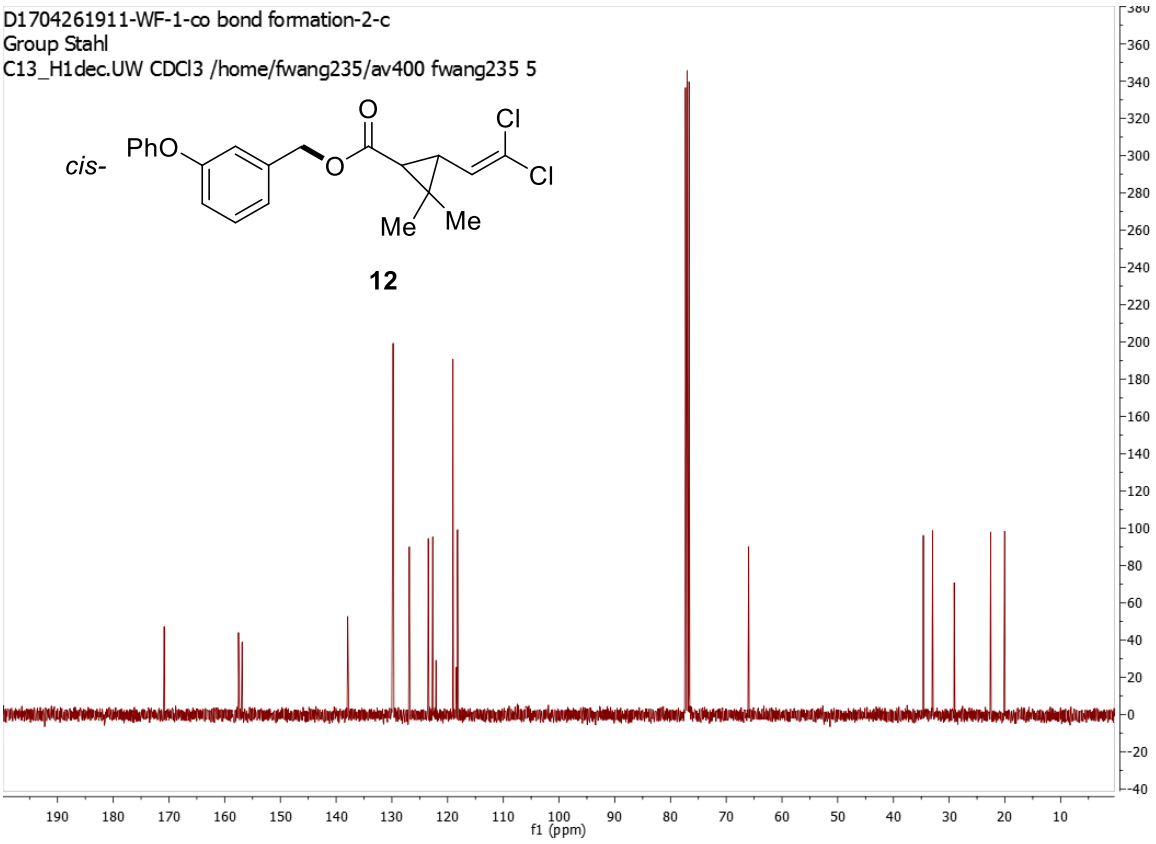
D1704261911-WF-1-co bond formation-2-c
Group Stahl
C13_H1dec.UW CDCl3 /home/fwang235/av400 fwang235 5
cis-
PhO
O
O
Cl
Cl
Me
Me
12
f1 (ppm)

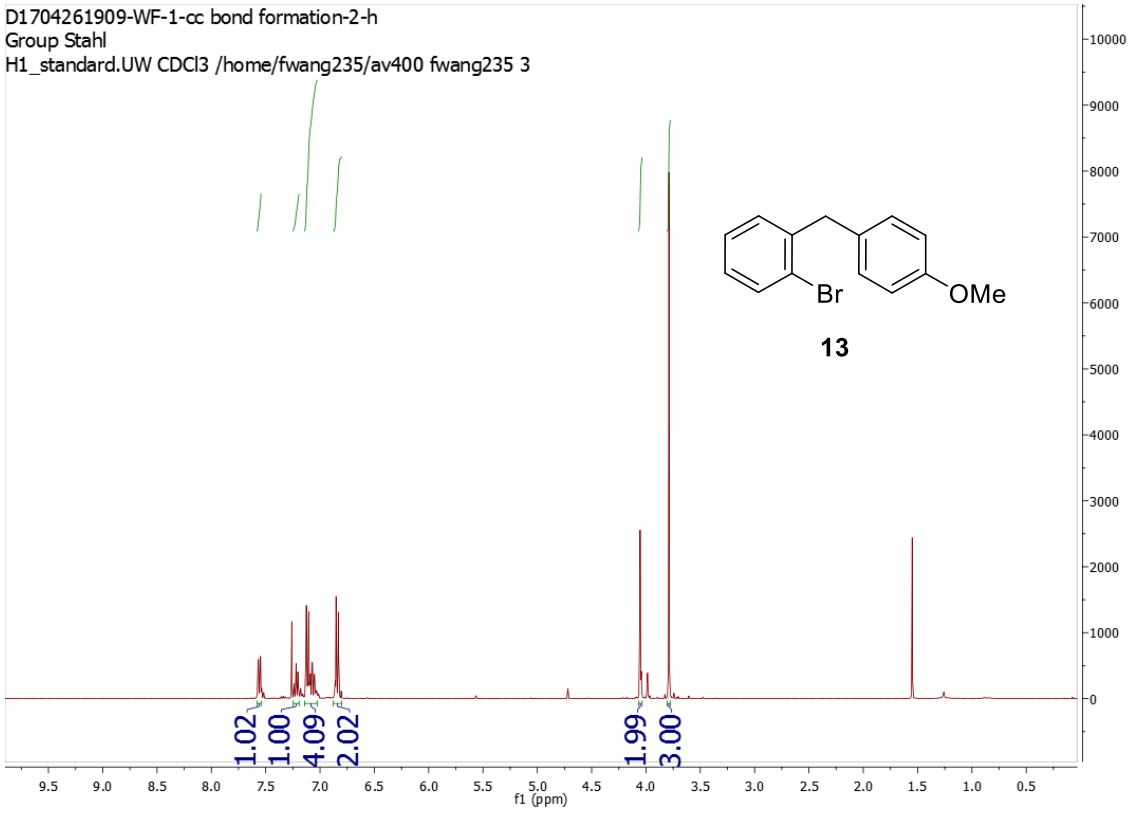
D1704261909-WF-1-cc bond formation-2-h
Group Stahl
H1_standard.UW CDCl3 /home/fwang235/av400 fwang235 3
Br
OMe
13
1.02
1.00
4.09
2.02
1.99
3.00
f1 (ppm)

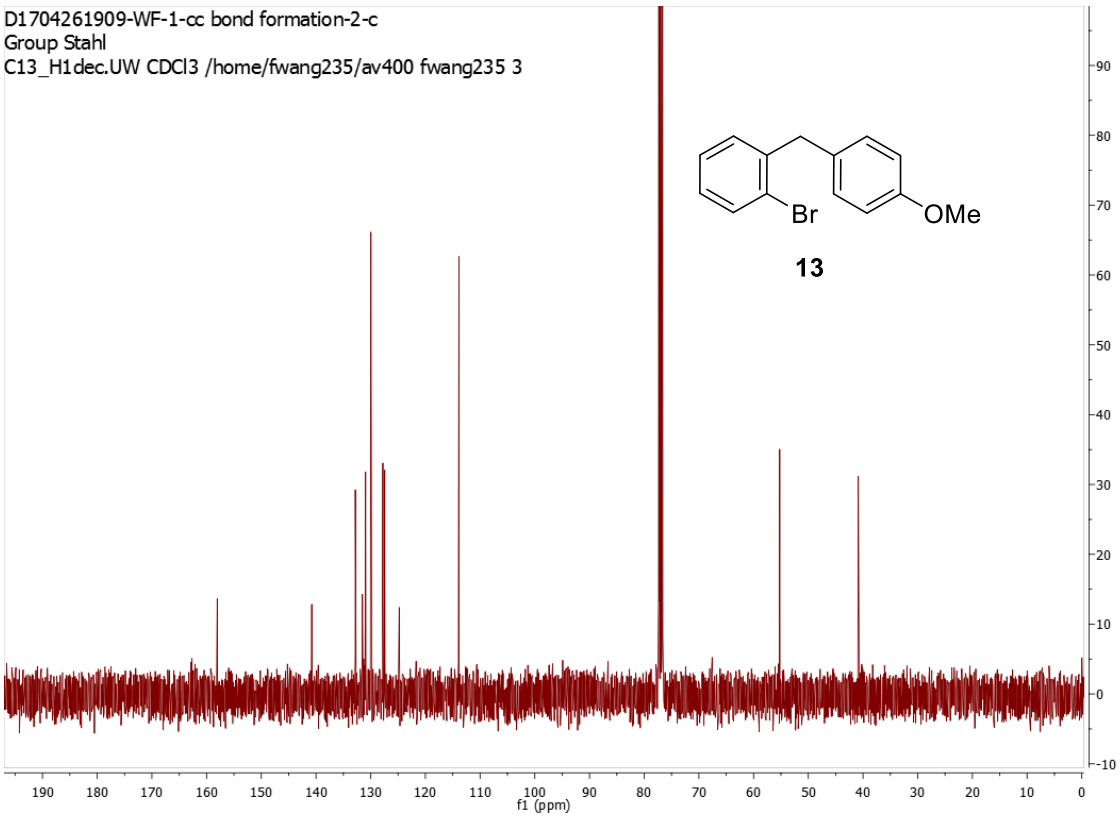
D1704261909-WF-1-cc bond formation-2-c
Group Stahl
C13_H1dec.UW CDCl3 /home/fwang235/av400 fwang235 3
Br
OMe
13
f1 (ppm)

10. References

1. Ohmori, H.; Takanami, T.; Shimada, H.; Masui, M. *Chem. Pharm. Bull.* **1987**, *35*, 2558.
2. Sasaki, K.; Newby, W. J. *J. Electroanal. Chem. Interfacial Electrochem.* **1969**, *20,* 137.
3. Brinkhaus, K.-H. G.; Steckhan, E.; Degner, D. *Tetrahedron* **1986***, 42,* 553.
4. Tajik, H.; Shirini, F.; Zolfigol, M. A.; Samimi, F. *Synth. Commun.* **2006**, *36*, 91.
5. Hosseinzadeh, R.; Tajbakhsh, M.; Lasemi, Z.; Sharifi, A. *Bull. Korean Chem. Soc.* **2004**, *25*, 1143.
6. Neuhaus, P.; Henkel, S.; Sander, W. *Aust. J. Chem.* **2010**, *63*, 1634.
7. Ruso, J. S.; Rajendiran, N.; Kumaran, R. S. *J. Korean Chem. Soc.* **2014**, *58*, 39.
8. Stoner, E. J.; Cothron, D. A.; Balmer, M. K.; Roden, B. A. *Tetrahedron* **1995**, *51*, 11043.
9. Moriya, T.; Yoneda, S.; Kawana, K.; Ikeda, R.; Konakahara, T.; Sakai, N. *J. Org. Chem.* **2013**, *78*, 10642.
10. Katritzky, A. R.; Bapat, J. B.; Blade, R. J.; Leddy, B. P.; Nie, P.-L.; Ramsden, C. A.; Thind, S. S. *J. Chem. Soc., Perkin Trans. 1*, **1979**, 418.
11 Rozwadowska, M. D.; Wysocka, W. *Pol. J. Chem.* **1982**, *56*, 533.
12. Sechi, M.; Bacchi, A.; Carcelli, M.; Compari, C.; Duce, E.; Fisicaro, E.; Rogolino, D.; Gates, P.; Derudas, M.; Al-Mawsawi, L. Q.; Neamati, N. *J. Med. Chem.* **2006**, *49*, 4248.
13. Bicker, W.; Kacprzak, K.; Kwit, M.; Lämmerhofer, M.; Gawronski, J.; Lindner, W. *Tetrahedron: Asymmetry* **2009**, *20*, 1027.
14. Corrie, T. J. A.; Ball, L. T.; Russell, C. A.; Lloyd-Jones, G. C. *J. Am. Chem. Soc.* **2017**, *139*, 245.